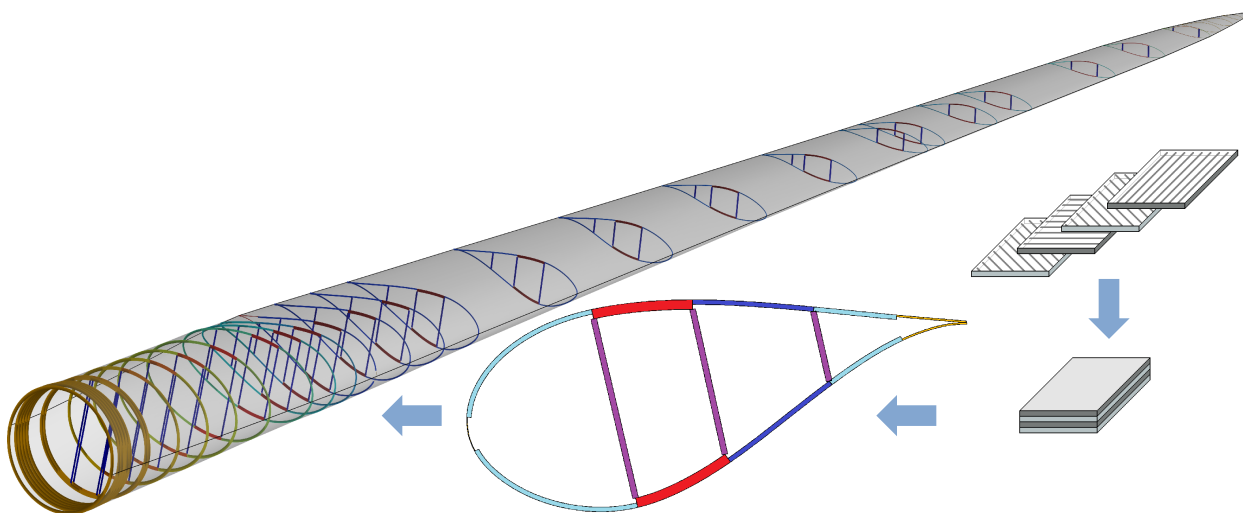


# User's Guide to Co-Blade: Software for Structural Analysis of Composite Blades

Danny C. Sale  
Northwest National Marine Renewable Energy Center  
Department of Mechanical Engineering  
University of Washington  
Seattle, WA



## 1. Introduction

Co-Blade is an engineering software used in the structural analysis and design of composite blades for wind and hydrokinetic turbines. The objective of Co-Blade is to help designers accelerate the preliminary design phase by providing the capabilities to rapidly evaluate alternative composite layups and to study their effects on composite blade properties and material stresses and strains.

Co-Blade computes span variant structural properties of composite blades which include: orientation of inertial/centroidal/elastic principal axes, extensional/torsional/bending stiffness, mass per unit span, mass moments of inertia, and offsets of the blade mass/tension/shear centers. Aeroelastic simulation codes (such as FAST [1], ADAMS, BLADED, etc.) require these structural properties as inputs to properly model the major flexible components of wind and hydrokinetic turbines—such as the blades and tower.

In addition to being a pre-processor for aeroelastic simulation codes, Co-Blade is a structural analysis tool capable of predicting the load induced blade deflections, lamina strains and stresses, and panel buckling stresses. Predictions of blade modal shapes and natural frequencies are also made possible by integrating the BModes code (a code developed for computing coupled mode shapes for rotating beams [2]) within Co-Blade. The methodology used within Co-Blade to compute structural properties and perform this structural analysis is based upon a combination of classical lamination theory with an Euler-Bernoulli theory and shear flow theory applied to composite beams. This approach allows for direct computation of structural properties and analysis, and it allows for Co-Blade to run very quickly (a single execution typically completes within several seconds or less). To further aid in the preliminary design of composite blades Co-Blade can also optimize the layup of composite materials within the blade using various optimization algorithms. For a given external blade shape and design load, Co-Blade can determine an optimal composite layup which minimizes the blade mass while simultaneously satisfying constraints on maximum stress, buckling, deflection, and placement of blade natural frequencies. Another motivation for developing Co-Blade was to integrate it with the rotor optimization code HARP\_Opt [3] to perform coupled aerodynamic and structural optimization of turbine blades.

This guide provides step-by-step instructions on how to prepare input data for Co-Blade, how to execute Co-Blade, and how to interpret the output results. The remaining sections of this guide cover the following topics:

- **Section 2 Installation of Co-Blade** describes the files included within the Co-Blade archive and installation procedure.
- **Section 3 Description of Composite Layup** explains the general types of composite blades that are possible to model using Co-Blade. An understanding of the convention that Co-Blade uses to construct composite blades is essential for preparing input data and interpreting the output.
- **Section 4 Technical Approach** describes the underlying theory implemented within Co-Blade and discusses some of the limitations and applicability of Co-Blade.
- **Section 5 Input Data Description** lists all the different types of input data files and provides instruction on how to specify external blade shape, applied loads, internal structural layup, and material properties.
- **Section 6 Executing Co-Blade** shows how to execute Co-Blade in both analysis and optimization modes.
- **Section 7 Output Data Description** explains how to interpret the Co-Blade output files.
- **Section 8 Conclusion & Future Work** discusses recommended verification studies and possible future work.
- **Appendix A** shows examples of figures that are created by Co-Blade. A large amount of data can be generated within the Co-Blade output files, and to assist in the post-processing of this output data Co-Blade includes options to generate many different 2D and 3D plots for instant visual feedback.

As a final note in this introductory section, we will highlight the similarities and differences between the PreComp [4] and Co-Blade codes. The PreComp code computes only the span variant properties of composites blades, and the Co-Blade code includes nearly all of the same capabilities of PreComp<sup>1</sup>, plus newly added analysis of load induced strain, stress, deflection, buckling, optimization capabilities, and graphical post-processing capabilities. PreComp and Co-Blade both apply a methodology based on the combination of classical lamination theory with an Euler-Bernoulli theory and shear flow theory applied to composite beams, but Co-Blade contains some minor differences and improvements on this methodology (which are further detailed in Section 4). And finally, the format of the input files to describe the external blade shape and structural layup established by the PreComp code have also been adopted by Co-Blade, allowing for existing PreComp models to be compatible with Co-Blade with little to no additional modifications.

---

<sup>1</sup> The only feature of PreComp v1.00.03 that is missing from Co-Blade is the computation of cross-coupled stiffness properties, which we hope to include in future versions of Co-Blade.

## 2. Installation of Co-Blade

Co-Blade was written in the MATLAB language and we have compiled a version of Co-Blade that can be used even if you do not own a version of MATLAB. The compiled version of Co-Blade is currently only supported on Windows operating systems. The Co-Blade source code has been written with cross-platform capability in mind, and it is possible that Co-Blade may run on Linux operating systems within MATLAB—although this has not currently been tested. To run the compiled version of Co-Blade you will need to first install the MATLAB Compiler Runtime (MCR). The MCR is a standalone set of shared libraries that enable execution of MATLAB scripts on computers without an installed version of MATLAB and associated licensing. The MCR is free and only needs to be installed once. Before running the compiled version of Co-Blade, you will need to install the MCR R2012a which is available for download at:

<http://www.mathworks.com/products/compiler/mcr/index.html>

Unless you want to make changes to the Co-Blade source code, you should only need to use the compiled version of Co-Blade. If you are developing for Co-Blade, all of the source code has also been included and the main MATLAB script is named *CoBlade.m*. The optimization capabilities of Co-Blade are dependent on both the “MATLAB Optimization Toolbox” and the “MATLAB Global Optimization Toolbox”. However, these toolboxes are required only when attempting to use Co-Blade in optimization mode—when run in analysis mode Co-Blade does not require any additional MATLAB toolboxes.

Unfortunately, the compiled version of Co-Blade runs significantly slower compared to running Co-Blade directly in MATLAB—this is because each time the compiled Co-Blade executable is run the MCR must be unpacked by the operating system which takes additional time (approximately 10-45 seconds are required just to unpack the MCR, while the execution of a single analysis of Co-Blade takes approximately 1-3 seconds).

To predict blade modal shapes and natural frequencies, the BModes code will also need to be installed (although this step is optional if modal analysis is not required). The BModes code is not included with Co-Blade, but it is freely available from the following website:

<http://wind.nrel.gov/designcodes preprocessors/bmodes/>

The following files are created upon extraction of the Co-Blade archive:

### ***working directory***

<i>Active_Input_Files.inp</i>	Text input file listing main input files which will be run by Co-Blade.
<i>CoBlade.exe</i>	The compiled Co-Blade executable file.
<i>CoBlade.m</i>	The main MATLAB script for Co-Blade.
<i>*.inp</i>	Example Co-Blade text input files.
<i>*.oup</i>	Example Co-Blade text output files.
<i>*.bmi</i>	Example BModes text input files, created automatically when Co-Blade runs.
<b> Airfoil_Data </b>	
<i>*.prof</i>	Example airfoil shape data text input files.
<b> Laminate_Data </b>	
<i>*.lam</i>	Example laminate data text input files.
<b> Material_Data </b>	
<i>*.inp</i>	Example material data text input files.
<b> Optimization_Data </b>	
<i>*.inp</i>	Example optimization text input files.
<b> Source </b>	
<i>*.m</i>	MATLAB source files.
<i>*.txt</i>	Licenses and documentations for source code.
<b> Documentation </b>	
<i>Co-Blade Users Guide.docx</i>	This user’s guide in MS Word format.
<i>Co-Blade Users Guide.pdf</i>	This user’s guide in PDF format.
<i>change_log.txt</i>	The list of changes made to Co-Blade for various versions.
<i>installation_instructions.txt</i>	Installation instructions for Co-Blade.
<i>*.mw</i>	Maple worksheet files containing some derivations of shear flow equations.

### 3. Description of Blade Composite Layup

Most modern blades, especially large turbine blades, are constructed from fiber-reinforced plastics (FRP) due to the superior strength-to-weight ratios of FRP compared to wood and metals. Figure 1 and Figure 2 illustrate examples of a composite blade (with an I-Beam and Box-Beam type layup, respectively) in which the primary bending loads are supported by the thick mid-sections (the spar caps) connected by one or more shear webs, and the aerodynamic shape is maintained by sandwich panels around the blade periphery. These types of composite blades are often constructed with stacks of laminas whose thickness, fiber orientation, and number are piecewise constant around a cross section periphery, while the number and thickness of the laminas will vary along the blade length. A laminate, defined as a stack of laminas, is distinguished by the number, sequence, fiber orientation, and material of the individual laminas in that stack. Note that even complicated composite layups, such as the blades illustrated in Figure 1 and Figure 2, are possible to model using Co-Blade.

Composite blades are frequently constructed using sandwich composite laminates. A basic sandwich composite laminate can be described as two thin and stiff FRP laminates separated by a thick core material with a low density. For composite turbine blades, popular fiber types include E-glass and carbon, and popular core materials include foam or balsa. The skin of the shell and webs are often constructed with multi-axial weave fibers for increased shear strength, while the spar caps contain large amounts of uni-directional fibers to provide the primary bending strength. The exterior surfaces of the laminates also frequently include a top coat to provide increased durability, a smooth surface, and to prevent moisture diffusion and fouling.

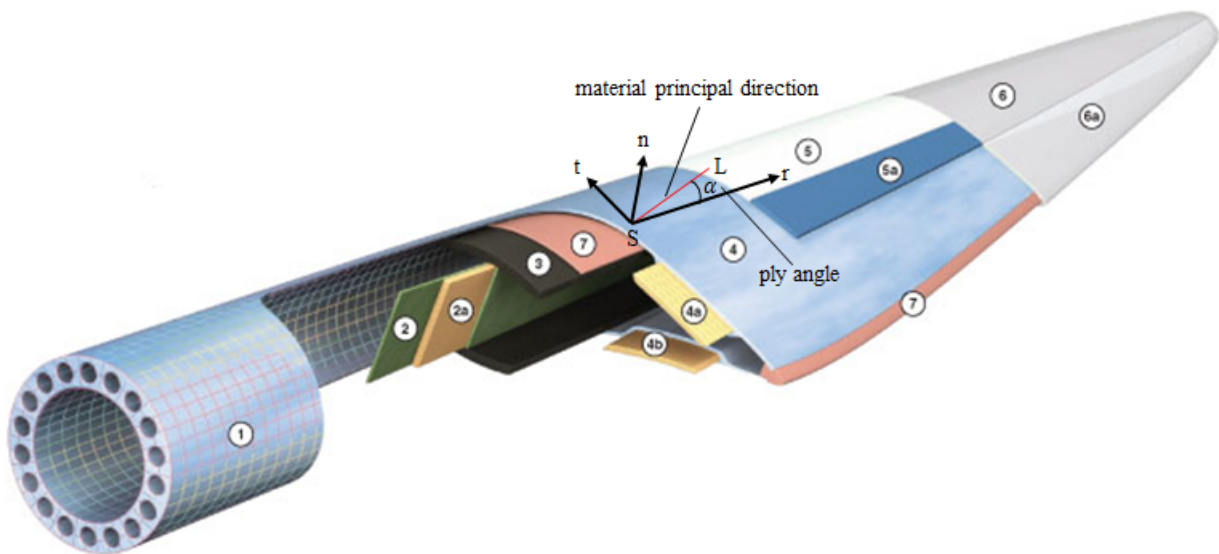


Figure 1. Illustration of a composite blade, showing the coordinate system used to orient the principal fiber directions. Material legend: (1) Root build-up, (2) Shear web shell, (2a) Shear web core, (3) Spar cap, (4) Blade shell, (4a/4b) Leading/Trailing Edge core, (5/5a) Priming gelcoats, (6/6a) Finishing gelcoats, (7) Structural adhesives. Image modified from original source: Gurit.com.

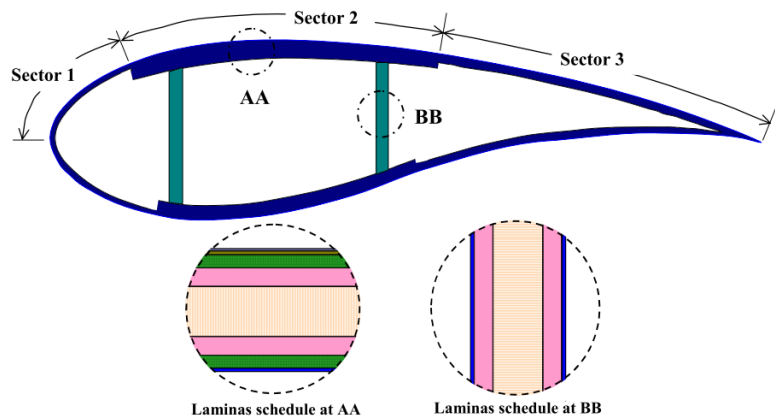


Figure 2. Illustration of a composite blade cross section. Image reproduced from [4].

### 3.1. Permissible Composite Layups

Figure 2 shows an example layup of a blade cross section with three laminates (identified by sectors 1-3) each on the upper and lower surfaces, with an additional two laminates for the shear webs. Co-Blade allows for an arbitrary number of laminates (consisting of an arbitrary configuration and number of materials) to be defined at each blade cross section, including an arbitrary number of shear webs (including zero). The shear webs may begin and end at any cross section, and the cross sectional dimensions and composite layup of the webs may also vary along the blade length. The webs are assumed to be located along the straight line connecting the web ends and are normal to the chord line at every cross section (which implies that if the blade includes pre-twist then the webs will be twisted as well).

Examples of permissible web geometries are shown in Figure 3. The webs are not permitted to cross each other. At any cross section the composite structural layup is assumed to be within the confines of the section external shape. The external shape at each cross section is characterized by its airfoil geometry, chord length, and aerodynamic pre-twist as illustrated in Figure 3 and Figure 4.

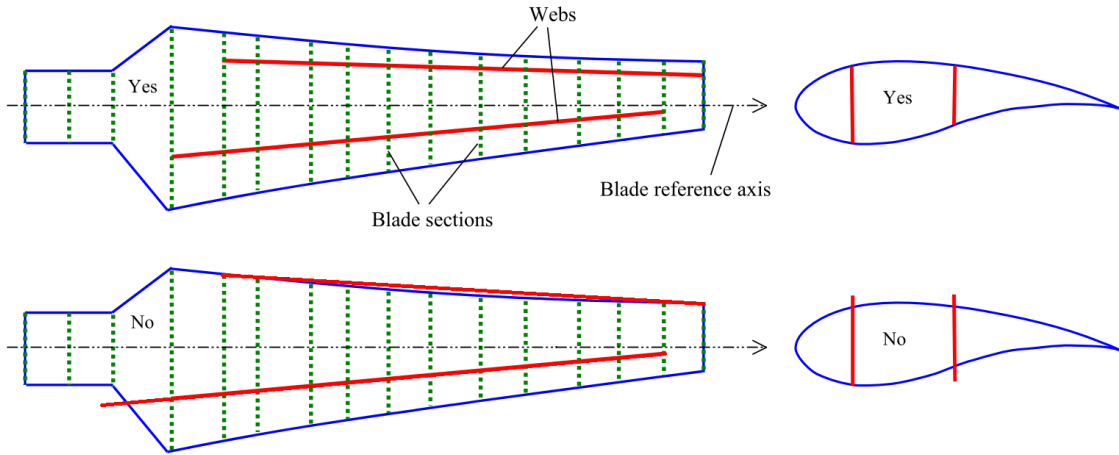


Figure 3. Cross sections may be located arbitrarily along the blade length. Each web must be within the confines of the external geometry and must originate at a cross section and terminate at an outboard cross section. Image modified from original source: [4].

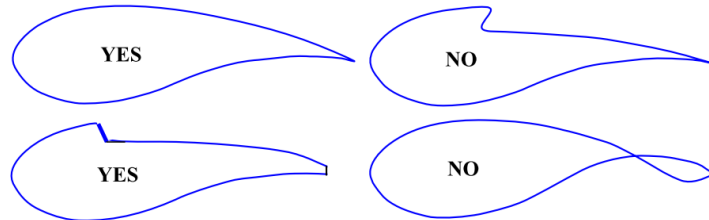


Figure 4. Illustration of permissible and non-admissible cross section airfoil shapes. Image reproduced from [4].

### 3.2. Optimization of Composite Layup

When using Co-Blade in analysis mode, it is possible to model a composite blade with nearly arbitrary topology and material properties, such as the blade illustrated in Figure 1. However, to perform a structural optimization Co-Blade is required to make some stricter assumptions about the blade composite layup in order to make the problem tractable. When Co-Blade is run in optimization mode the layup of composite materials is restricted to the configuration illustrated in Figure 5 and Figure 6. As Figure 5 and Figure 6 show, the blade consists of 9 unique laminate schedules with a total of 8 materials (where each material can have its own unique properties). A description of the laminates within each section of the blade is as follows:

- **“root build-up”:** The thick “blade-root” material is sandwiched between the “blade-shell” material. A large material thickness at the blade root is often required to accommodate metal threaded inserts for attachment of the blade to the rotor hub. The thickness of the “blade-root” material linearly decreases moving towards the maximum chord blade

station, while the thicknesses of the LEP, TEP, and spar cap materials begin to increase linearly. Near the maximum chord blade station, the “blade-root” material has tapered off completely, and the thicknesses in the LEP, TEP, and spar cap have reached their maximum.

- **“leading edge panel (LEP)”:** The material schedule is [“blade-shell” / “blade-root” / “LEP-core”]<sub>s</sub>.
- **“trailing edge panel (TEP)”:** The material schedule is [“blade-shell” / “blade-root” / “TEP-core”]<sub>s</sub>.
- **“spar cap”:** The material schedule is [“blade-shell” / “blade-root” / “spar-uni” / “spar-core”]<sub>s</sub>.
- **“shear web”:** The “web-core” material is sandwiched between the “web-shell” material.
- **“blade tip”:** at the blade tip, all other lamina plies have been dropped and only the “blade-shell” material exists. Note, the “blade-shell” material covers the interior and exterior surfaces of the top and bottom blade surfaces along the entire length of the blade.

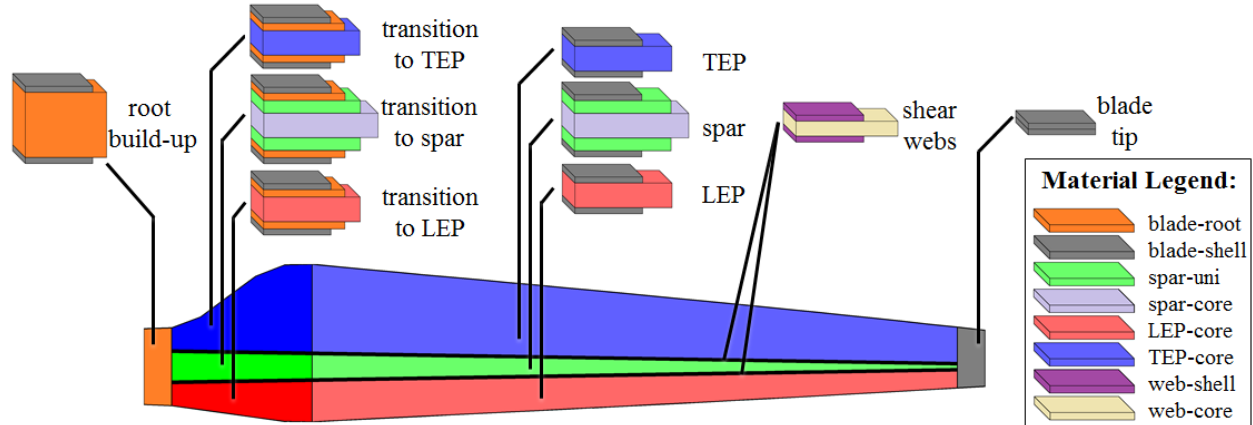


Figure 5. Illustration of the composite layup when Co-Blade is run in optimization mode. The blade is shown in planform view, illustrating the laminate material schedules in the root build-up, leading edge panel (LEP), spar cap, trailing edge panel (TEP), shear webs, and blade tip.

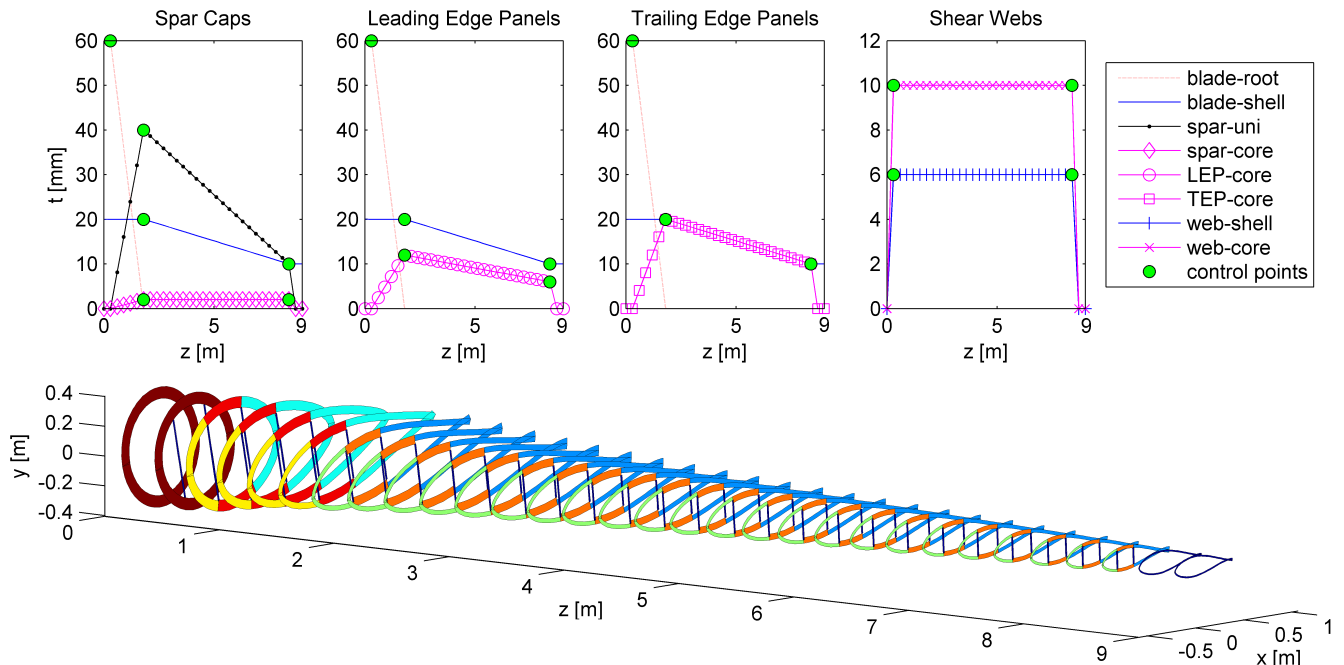


Figure 6. An example of how the thickness ( $t$ ) of the different materials varies along the blade length ( $z$ ) when Co-Blade is run in optimization mode. The material thicknesses vary linearly between the control points, which remain at user-specified fixed stations. The laminate material schedule is identical to that illustrated in Figure 5, and the thickness ( $t$ ) represents the *total* material thickness in the symmetric laminates.

In optimization mode, the laminate schedules and chordwise subdivisions of laminates are identical on the top and bottom blade surfaces, and the laminates of the shear webs are identical to each other. All laminates are balanced and symmetric, eliminating the possibility for cross-coupled stiffnesses. The ends of the spar caps and shear webs remain fixed at user specified inboard and outboard stations, but the optimization algorithm can vary the chordwise locations of the spar caps and shear webs. The chordwise locations of the spar cap and shear webs are also positioned to be symmetric about the blade pitch axis. In order to use continuous design variables, each lamina is modeled as a single ply with continuously variable thickness, as opposed to a stack of multiple plies with discrete thicknesses.

The design variables are the chordwise width of the spar cap at the inboard and outboard locations, the thickness of the “blade-root” material, and the thicknesses of the laminas within the LEP, TEP, spar cap, and shear webs along the length of the blade. Figure 6 shows how the material thicknesses in the LEP, TEP, spar cap, and shear webs vary along the length of the blade. As shown in Figure 6, the thickness of each material along the length of the blade is defined by the linear variation between control points. In order to achieve a more general variation of thickness along the blade length than the example shown in Figure 6, the user can specify the total number of control points (which are equally spaced along the blade length between the TRAN\_STN and OUB\_STN blade stations)—this will be further explained in Table 2 of Section 5.2.

As Figure 6 shows, the “blade-root” material exists only between the first blade station and the blade station defined by TRAN\_STN. The “blade-root” material is constant in thickness inboard of the INB\_STN blade station and then decreases linearly to zero between the INB\_STN and TRAN\_STN blade stations. The thickness of the “blade-shell” material remains constant inboard and outboard of the blade stations defined by INB\_STN and OUB\_STN, and varies linearly between the control points defined between the INB\_STN and OUB\_STN blade stations. The “LEP-core”, “TEP-core”, “spar-uni”, and “spar-core” materials exist only between the INB\_STN and OUB\_STN blade stations—and the thicknesses of these materials increase linearly from 0 to their maximum value between the INB\_STN and TRAN\_STN blade stations, and then vary linearly between the control points defined between the TRAN\_STN and OUB\_STN blade stations. The “web-shell” and “web-core” materials exist only between the INB\_STN and OUB\_STN blade stations, and the thickness of these materials vary linearly between the control points at the INB\_STN and OUB\_STN blade stations.

## 4. Technical Approach

A full discussion of the technical approach implemented within Co-Blade is outside the scope of this manual. However, a brief outline of the underlying theory and references to some helpful texts which discuss relevant methods and theories in greater detail will be provided. The underlying theory implemented within Co-Blade is based upon a combination of classical lamination theory (CLT) with an Euler-Bernoulli theory and shear flow theory applied to composite beams. First, the turbine blade is represented as a cantilever beam which undergoes flapwise bending, edgewise bending, axial deflection, and elastic twist. Additional coupling between bending, extension, and torsion are accounted for through offsets of the beam shear center, tension center, and center of mass from the blade pitch axis. The beam cross sections are thin-walled, closed, and single- or multi-cellular. The periphery of each beam cross section is discretized as a connection of flat composite laminates, as illustrated in Figure 7. The mechanical properties of the composite laminates are computed using classical lamination theory, which is well described in texts such as [5, 6]. Although each laminate is actually an assembly of multiple fibrous composite materials (where each layer can have significantly different constitutive properties), classical lamination theory can be used to calculate a set of “effective” mechanical properties which essentially allows a multi-layered composite plate to be treated as a single structural element.

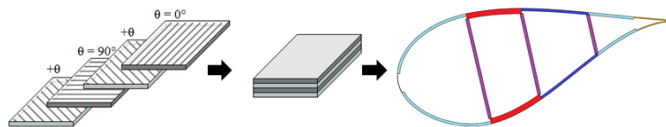


Figure 7. The blade cross sections are discretized as a connection of composite laminated plates.

Now in view of Euler-Bernoulli beam theory, the beam cross sections are heterogeneous; i.e., the material properties are dependent on the location within the composite beam cross section. In this case the composite beam is composed of discrete portions of homogenous make-up, where each discrete portion of the composite beam is characterized by the effective mechanical properties computed via CLT. Each discrete portion of the cross section then contributes to the global section properties of the composite beam, which are computed as modulus weighted section properties (described further in [7, 8]). Knowing the global cross sectional properties, the deflections and effective beam axial stress ( $\sigma_{zz}$ ) and effective beam shear stress ( $\tau_{zs}$ ) are now computed under the assumptions for an Euler-Bernoulli beam (again see [7, 8, 9]). The calculation of  $\tau_{zs}$ , prediction of shear center and torsional stiffness is based on a shear flow approach which follows similarly from [9].

Finally, by converting the distribution of effective beam stresses  $\sigma_{zz}$  and  $\tau_{zs}$  into equivalent in-plane distributed loads on the flat laminates which idealize the cross section periphery (as shown in Figure 8), the lamina-level strains and stresses in the principal fiber directions ( $\varepsilon_{11}$ ,  $\varepsilon_{22}$ ,  $\gamma_{12}$ ,  $\sigma_{11}$ ,  $\sigma_{22}$ , and  $\tau_{12}$ ) can be recovered using CLT.

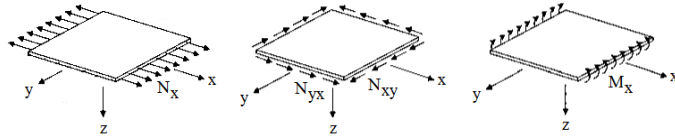


Figure 8. The effective beam stresses from Euler-Bernoulli theory are converted to equivalent extensional, shear, and bending loads on a composite laminated plate so that the lamina level stresses and strains can be recovered.

Co-Blade performs a linear buckling analysis to predict the critical buckling stresses following the approach of [10, 11]. In this approach, Co-Blade idealizes the top and bottom surfaces of the blade as curved plates subjected to the combined conditions of compression and shear. The shear webs are idealized as flat plates subjected to the combined conditions of bending and shear. Figure 9 illustrates the loading conditions used to predict the critical buckling stresses. The plates are idealized as isotropic and having simply-supported (pinned) boundary conditions on all four sides (which is a conservative approach). The plate stiffness (effective stiffness from CLT), thickness, curvature, and width dimensions therefore contribute to the prediction of critical buckling stresses.

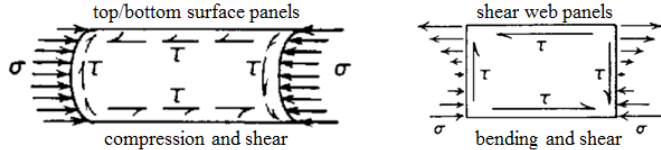


Figure 9. For the linear buckling analysis, the top and bottom surfaces of the blade are modeled as curved plates subjected to combined compression and shear. The blade shear webs are modeled as flat plates subjected to combined bending and shear.

The predictions of beam natural frequencies and modal shapes are provided by the BModes code, and the reader is referred to [2] for further detail. In summary, BModes formulates energy expressions and uses Hamilton's principle to derive a set of nonlinear coupled integro-partial differential equations (PDEs) which govern the dynamics of an Euler-Bernoulli beam. BModes discretizes these PDEs using specialized 15 degree-of-freedom finite elements, and then performs an eigenanalysis to obtain the coupled mode shapes and frequencies.

The underlying theory within Co-Blade is based on a number of assumptions, which are required to make this structural analysis tractable:

1. Each blade section is a thin-walled, closed, single- or multi-cellular section. Unlike the PreComp code [4], Co-Blade does not assume that shear flow is constant around each cell.
2. For the calculations of effective beam stresses and centroidal displacements, Co-Blade uses an Euler-Bernoulli composite beam model, which assumes:

- a. The cross sections of the composite blade consist of discrete areas of homogenous material (these discrete areas are referred to as panels). Each panel is characterized by its effective Young's modulus, effective shear modulus, effective Poisson's ratio, thickness, and density as computed from classical lamination theory. The method of modulus weighted properties is used to compute the global cross section properties of the composite beam.
  - b. The transverse components of beam normal stress ( $\sigma_{xx}$  and  $\sigma_{yy}$ ) are negligible compared to the beam axial stress ( $\sigma_{zz}$ ).
  - c. Cross sections are assumed to remain planar and normal to the centroidal axis of deformation (i.e. the axis which passes through the locus of tension centers).
  - d. The Euler-Bernoulli beam equations in their commonly published form assume small deflections and uniform cross sections. Co-Blade applies a correction factor, following the approach of [11] and validated in [12], to the beam deflection equations to account for tapered beams.
3. The panel critical buckling stresses are computed by modeling the panels as thin plates with a pinned boundary condition on all edges of the plate. This type of boundary condition is conservative, and is likely to lead to over-designs of the panel thickness:
- a. For the panels on the top and bottom surfaces, Co-Blade computes the panel critical buckling stress for a curved thin plate under the combined effects of compression and shear. The effective beam compressive normal stress and shear stress are averaged over each panel.
  - b. For the shear webs, Co-Blade computes the panel critical buckling stress for a straight thin plate under the combined effects of bending and shear. In this case, the minimum compressive normal stress and panel averaged shear stress are applied in the buckling analysis.
4. For the calculations of *lamina* strains and stresses ( $\varepsilon_{11}$ ,  $\varepsilon_{22}$ ,  $\gamma_{12}$ ,  $\sigma_{11}$ ,  $\sigma_{22}$ , and  $\tau_{12}$ ), the effective beam normal stress ( $\sigma_{zz}$ ) and effective beam shear stress ( $\tau_{zs}$ ) are converted into equivalent thin plate loads. The strains and stresses at the lamina level are computed under the assumptions of classical lamination theory.
5. The modal calculations provided by the BModes code [2] are performed with zero damping.

## 5. Input Data Description

The following information will need to be provided by the user in order for Co-Blade to compute beam structural properties and perform a complete structural analysis:

1. Description of blade external shape, which is defined by:
  - a. blade length
  - b. chord, pre-twist, and section airfoil geometry distribution along the blade
  - c. pitch-axis distribution along the blade (Co-Blade can also determine an optimal pitch-axis distribution if this data is unavailable)
2. Description of blade internal structure, which is defined by:
  - a. number and placement of distinct laminates along the blade periphery
  - b. number and placement of shear webs within the blade
  - c. lamina schedules for the laminates along the blade periphery and shear webs
3. Table of material properties, which include:
  - a. elastic and shear modulii, Poisson ratio, and density
  - b. failure and yielding stresses
4. Description of applied loads and rotor operating conditions, which include:
  - a. applied aerodynamic forces and moments
  - b. rotor shaft tilt, blade azimuth, blade pre-cone, and blade pitch angles
  - c. rotor rotational speed and blade hub radius
5. Description of design constraints, which include:
  - a. material maximum allowable stresses
  - b. blade maximum allowable deflection
  - c. range of allowable blade natural frequencies

The required input data, described above, is provided via 5 sets of text input files: a main input file, airfoil shape data files, laminate data files, a materials data file, and optimization input files. A set of example input files is also included with Co-Blade and it is recommended to modify these example files to suit your needs. All input files are written in a simple text format that can be created or modified with any text editor. Instructions on how to create and interpret each of these input files is given in the following sections.

### 5.1. Coordinate Systems

Prior to creating the required input data and interpreting the output data files, it is helpful to understand the different coordinate systems used within Co-Blade:

#### Global Coordinate System

- note: this is the reference global coordinate system, it does not ever move  
origin: (0,0,0), the apex of the cone of rotation  
+x-dir: points in the downstream direction of the nominal free stream  
+y-dir: orthogonal to global x-z axes, forms a right handed coordinate system  
+z-dir: pointing vertically upward, opposite the direction of gravity

#### Shaft Coordinate System

- note: this system rotates with the rotor  
origin: same as the global coordinate system, the apex of the cone of rotation  
+x-dir: points in the downstream direction of the possibly tilted shaft  
+y-dir: orthogonal to shaft x-z axes, forms a right handed coordinate system  
+z-dir: points in the direction of blade azimuth

#### Blade Coordinate System

- note: this system rotates with the blade azimuth, and rotates with the blade pitch  
origin: intersection of the blade pitch axis and the blade root  
+x-dir: points in the direction of the airfoil trailing edge parallel with the chord line as if there was zero pre-twist of the blade. In other words, this axis is the line which is both orthogonal to the blade pitch axis and also tangent to the cone of rotation's surface.  
+y-dir: orthogonal to blade x-z axes, forms a right handed coordinate system  
+z-dir: the blade pitch axis, pointing towards the blade tip

The structural properties computed by Co-Blade are defined with respect to the axes shown in Figure 10. The reference plane is the same as the x-axis of the blade coordinate system. The angle  $\theta_{\text{aero}}$  (`aeroTwst`) is the aerodynamic twist that defines

the orientation of the chord line at each blade station with respect to the reference plane.  $X_R$ - $Y_R$  are the section reference axes with origin at R, which is the intersection of the section reference axes with the blade pitch axis. The  $X_R$  axis points towards the trailing edge and coincides with the section chord line. The angle  $\theta_{\text{centroidal}}$  ( $\text{cent\_tw}$ ) defines the orientation between the reference plane and the centroidal principal axes  $X_{tc}$ - $Y_{tc}$  which have origin at the tension center (TC). The angle  $\theta_{\text{inertial}}$  ( $\text{iner\_tw}$ ) defines the orientation between the reference plane and the inertial principal axes  $X_{cm}$ - $Y_{cm}$  which have origin at the center of mass (CM). The angle  $\theta_{\text{elastic}}$  ( $\text{elas\_tw}$ ) defines the orientation between the reference plane and the elastic principal axes  $X_{sc}$ - $Y_{sc}$  which have origin at the shear center (SC). The x-axes and y-axes of these coordinate systems are also referred to as the flapwise and edgewise axes, respectively.

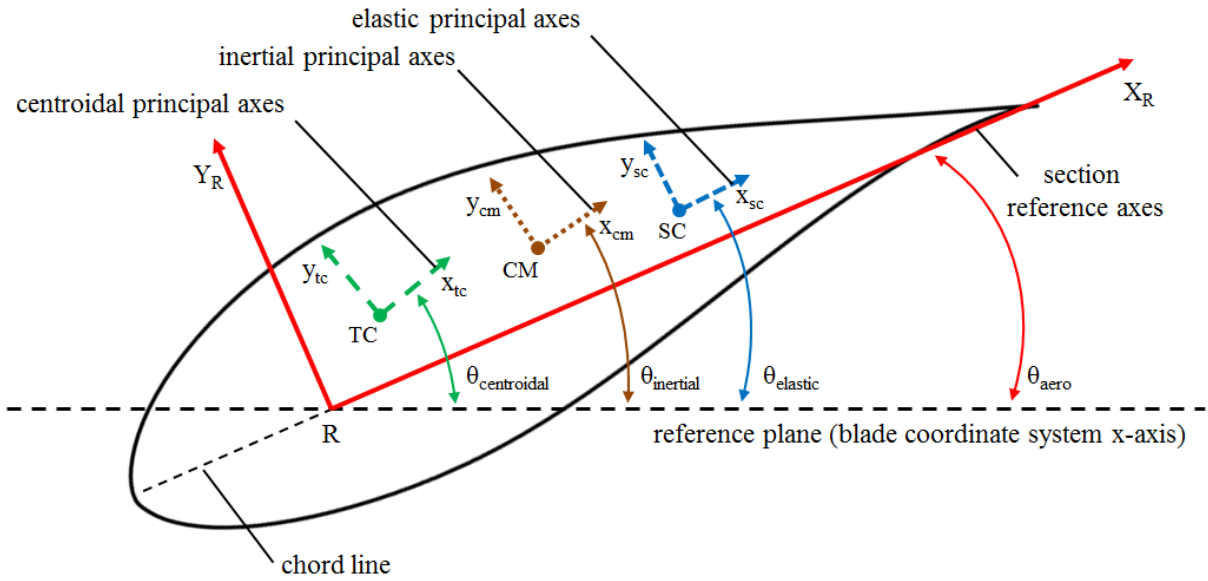


Figure 10. Orientation of the different axes within each cross section.

## 5.2. Main Input File

The main input file can have any name, but it should have the file extension *.inp*. Two examples of a main input file have been included with Co-Blade: *TidalTurbineRef.inp* and *WindTurbineRef.inp*. The main input file contains several blocks of input parameters which are described in Tables 1-7.

Table 1. Main Input File “Analysis Options” Parameters

Parameter	Description
SELF_WEIGHT	A logical switch. If set to <i>true</i> , the net weight of the blade will be included as a body force.
BUOYANCY	A logical switch. If set to <i>true</i> , the effect of buoyancy will be included in the net weight body force.
CENTRIF	A logical switch. If set to <i>true</i> , the centrifugal force will be included as a body force.
DISP_CF	A logical switch. If set to <i>true</i> , correction factors for displacement of a tapered cantilevered beam will be applied to the transverse centroidal displacements.
N_MODES	A positive integer. The number of modes that will be computed. This number can be zero if you do not wish to perform a modal analysis.
N_ELEMS	A positive integer. Number of blade finite elements used in the BModes modal analysis.

Table 2. Main Input File “Optimization” Parameters

Parameter	Description
OPTIMIZE	A logical switch. If set to <i>true</i> , Co-Blade will optimize the layup of composite materials in the blade, as described in Section 3.2, in order to minimize the fitness function $f(\vec{x})$ as described in Section 6.3. If set to <i>false</i> , the remainder of input parameters in this section are ignored, except for OPT_PITAXIS and PITAXIS_VAL.
OPT_METHOD	This flag selects which optimization algorithm is used to perform optimization of the composite layup. Accepted inputs are “PS” for Pattern Search, “GS” for Gradient Search, and “PSO” for Particle Swarm Optimization. Further options for each optimization algorithm can be set in the auxiliary input files: <i>PatternSearchOptions.inp</i> , <i>GradientSearchOptions.inp</i> , and <i>ParticleSwarmOptions.inp</i> located in the <i>\Optimization_Data</i> folder.
OPT_PITAXIS	A logical switch. If set to <i>true</i> , Co-Blade will ignore the currently entered values for pitAxis (the pitch axis) and determine new values for pitAxis between the first blade station and the maximum chord blade station. Outboard of the maximum chord station pitAxis will take on the value entered for PITAXIS_VAL, but inboard of the max chord station the values of pitAxis will be optimized to minimize the curvature of the blade leading and trailing edges.
PITAXIS_VAL	If OPT_PITAXIS is <i>true</i> , this value will be used for pitAxis outboard (and including) the maximum chord blade station. This value is ignored if OPT_PITAXIS is <i>false</i> .
INB_STN	A positive integer. Inboard blade station where the leading and trailing edge panels, spar caps, and shear webs begin. See Figure 6.
TRAN_STN	A positive integer. Blade station where the leading and trailing edge panels and spar caps reach their maximum thickness after transitioning from zero thickness at INB_STN. The “blade-root” material tapers from its maximum thickness at INB_STN to zero thickness at TRAN_STN. See Figure 6.
OUN_STN	A positive integer. Outboard blade station where the leading and trailing edge panels, spar caps, and shear webs end. See Figure 6.
NUM_CP	A positive integer. The number of control points used to define the lamina thicknesses of the “LEP-core”, “TEP-core”, “spar-uni”, “spar-core”, and “blade-shell” materials along the length of the blade. The radial locations of the control points for these materials are spaced evenly between the TRAN_STN and OUN_STN blade stations. The shear web lamina thicknesses are always defined using only two control points, located at INB_STN and OUN_STN. See Figure 6.
READ_INITX	A logical switch. If set to <i>true</i> , the initial values of the design variables are read from the file specified by INITX_FILE —two examples of this file are provided in the <i>\Optimization_Data</i> folder. This file allows you to enter initial values for the design variables, and the parameters in this file are described in Table 11 of Section 5.6.
INITX_FILE	Name of the file where the initial values of the design variables (see Table 11) are stored. This file can have any name, but it must have the .inp file extension and should be located in the <i>\Optimization_Data</i> folder.
WRITE_STR	A logical switch. If set to <i>true</i> , the laminate input text files are written at each function evaluation. (recommend to set <i>false</i> unless for debugging purposes.)
WRITE_F_ALL	A logical switch. If set to <i>true</i> , the fitness value and penalty factors are written to a text file at each function evaluation. (recommend to set <i>false</i> unless for debugging purposes.)
WRITE_X_ALL	A logical switch. If set to <i>true</i> , the values of the design variables are written to a text file at each function evaluation. (recommend to set <i>false</i> unless for debugging purposes.)
WRITE_X_ITER	A logical switch. If set to <i>true</i> , the current values of the design variables are written to a text file at each iteration. (recommend to set <i>false</i> unless for debugging purposes.)

Table 3. Main Input File “Environmental Data” Parameters

Parameter	Description
FLUID_DEN	Fluid density which the blade is operating in. Units [kg/m <sup>3</sup> ].
GRAV	Acceleration due to gravity. Units [m/s <sup>2</sup> ].

Table 4. Main Input File “Constraints” Parameters

Parameter	Description
MAX_TIP_D	The maximum allowable tip deflection. Tip deflection is defined as the deflection at the blade tip in the direction of the tower (computed as the displacement in the x-direction of the global coordinate system). Units [m].
MIN_FREQ_SEP	Minimum allowable difference between the blade rotation frequency and the blade natural frequencies. Units [Hz].

Table 5. Main Input File “Blade Data” Parameters

Parameter	Description
NUM_SEC	A positive integer. Total number of blade cross sections.
BLD_LENGTH	The length of the blade, measured along the coned radius from the blade root to blade tip. Units [m].
HUB_RAD	The hub radius, measured along the coned radius from the apex of the cone of rotation to the blade root. Units [m].
SHAFT_TILT	This is the tilt angle of the rotor shaft from the nominally horizontal plane. Positive tilt is defined such that the downstream end of the shaft is closer to the ground. This value must be between -90 and 90 degrees. Upwind turbines typically have a positive shaft tilt for greater tower clearance. A positive shaft tilt angle produces a positive right-handed rotation about the y-axis of the global coordinate system. Units [deg].
PRE_CONE	The blade pre-cone angle. Upstream turbines typically define a negative pre-cone angle for greater tower clearance, although this also increases the blade bending moments. Downstream turbines typically define a positive pre-cone angle to counter-act blade bending moments. The pre-cone angle must be defined within the range $-180^\circ < \text{PRE\_CONE} < 180^\circ$ . A positive pre-cone angle produces a positive right-handed rotation about the y-axis of the shaft coordinate system. Units [deg].
AZIM	The blade azimuth angle. Looking downstream, the azimuth angle is defined in a clock-wise fashion with $0^\circ$ defined at the "12-o-clock" position. A positive azimuth angle produces a positive right-handed rotation about the x-axis of the shaft coordinate system. Units [deg].
BLD_PITCH	The blade pitch angle. A positive blade pitch angle produces a positive right-handed rotation about the z-axis of the blade coordinate system. Units [deg].
ROT_SPD	The rotor rotational speed. Units [rpm].
INTERP_AF	This flag can be used to alter the number and spacing of analysis nodes along the perimeter of the airfoil. Accepted inputs are <i>none</i> , <i>cosine</i> , or <i>equal</i> . If <i>none</i> is selected, the number and location of the nodes along the airfoil perimeter will exactly match the values defined in the airfoil input files. If <i>cosine</i> is selected, the node locations will be interpolated from the node locations defined in the airfoil input files to have a chordwise spacing with a cosine distribution, with higher density of nodes near the leading and trailing edges. If <i>equal</i> is selected, the airfoil node locations will be interpolated to have an equal chordwise spacing.
N_AF	A positive integer. The total number of interpolated analysis nodes along the airfoil perimeter. Ignored if INTERP_AF is set to <i>none</i> .

MATS_FILE	Name of the file where the materials data is stored. This file can have any name, but it must have the .inp file extension and it should be placed in the \Materials_Data folder.
FILLER_DENS	Density of the blade filler material. If non-zero, all hollow regions within the blade are assumed to be filled with this material. Some blade designs use a foam or epoxy slurry as a filler material to help resist buckling. Hydrokinetic turbine blades might use a filler material to make the blades approximately neutrally buoyant. (THIS VALUE IS CURRENTLY IGNORED) Units [kg/m <sup>3</sup> ].
zFrac	This column of data is the span location of the blade cross sections measured from the blade root and normalized by the blade length. The first cross section is always located at zFrac = 0.0 and the last at zFrac = 1.0. The total number of cross sections and number of entries for zFrac is equal to NUM_SEC.
aeroTwst	This column of data is the aerodynamic pre-twist of each cross section. This represents the orientation of the chord line at each cross section with respect to the reference plane (see Figure 10). A positive aerodynamic pre-twist produces a positive right-handed rotation about the pitch axis (the z-axis of the blade coordinate system). Units [deg].
chord	This column of data is the chord length at each cross section. Units [m].
pitAxis	This column of data is the pitch axis of the blade, defined as the distance along the chord line from the leading edge of the chord normalized by the chord length. It is a value between 0 and 1.
px_a	This column of data is the distributed aerodynamic force per unit length applied along the pitch axis in the x-direction of the blade coordinate system. Units [N/m].
py_a	This column of data is the distributed aerodynamic force per unit length applied along the pitch axis in the y-direction of the blade coordinate system. Units [N/m].
qz_a	This column of data is the distributed aerodynamic moment per unit length applied along the pitch axis, defined as a right-handed rotation about the z-axis of the blade coordinate system. Units [N].
af_shape_file	For each blade station entered in this table, an auxiliary input file which describes the external shape must be supplied (see the following section for the “Airfoil Shape Input File”). The same airfoil shape input file can be supplied for multiple sections. For example, if the airfoil shape input file NACA6_0240.prof is supplied for stations 10 – 31, this implies that these stations all have the same external shape defined by the input file NACA6_0240.prof.
int_str_file	For each blade station entered in this table, an auxiliary input file which describes the internal structure of the cross section must also be supplied. Multiple stations can be described by the same laminate input file. For example, if the laminate input file example_1-12.lam is supplied for stations 1 – 12, this implies that these stations all have the same internal structural layup defined by the laminate input file example_1-12.lam.

Table 6. Main Input File “Shear Web Data” Parameters

Parameter	Description
NUM_WEBS	A positive integer. The total number of shear webs within the blade. Each web is defined along a straight line between its inboard and outboard ends, and perpendicular to the chord line at each station. It is also permissible to set NUM_WEBS = 0 if no shear webs exist. If OPTIMIZE is set to true, NUM_WEBS must be greater than 0 and the shear webs are equally spaced along the chord line between the leading and trailing edges of the spar cap.
WEB_NODES	A positive integer. The number of analysis nodes within each shear web. Since the shear webs are always straight any small number (greater than 3) should be sufficient.
webNum	A positive integer. This column of data is the web identification number. The first web is assumed to be the web closest to the leading edge and subsequent webs are defined aft of the first web. Shear webs are not allowed to cross each other. This value ignored if OPTIMIZE is set to true.

inbStn	A positive integer. This column of data is the blade station at which the inboard end of the web is located. This value ignored if OPTIMIZE is set to <i>true</i> .
oubStn	A positive integer. This column of data is the blade station at which the outboard end of the web is located. This value ignored if OPTIMIZE is set to <i>true</i> .
inbChLoc	This column of data defines the chordwise location of the web at the inboard station. The chordwise location is measured from the leading edge and is normalized by the chord length. This value ignored if OPTIMIZE is set to <i>true</i> .
oubChLoc	This column of data defines the chordwise location of the web at the outboard station. The chordwise location is measured from the leading edge and is normalized by the chord length. This value ignored if OPTIMIZE is set to <i>true</i> .

Table 7. Main Input File “Output Options” Parameters

Parameter	Description
TAB_DEL	A logical switch. Setting TAB_DEL to <i>true</i> tells Co-Blade to generate the text output files with tabs between the columns, instead of using fixed format. Tab-delimited files are best for importing into spreadsheets, while fixed-format files are best for viewing with a text editor or for printing.
PROPS_FILE	A logical switch. Setting PROPS_FILE to <i>true</i> tells Co-Blade to generate the structural properties output file. The structural properties output file contains the computed principal axes, stiffnesses, mass, mass moments of inertia, and centers of mass, tension, and shear. Table 12 of Section 7 explains how to interpret the data in the structural properties output file.
LOAD_DSP_FILE	A logical switch. Setting LOAD_DSP_FILE to <i>true</i> tells Co-Blade to generate the loads and displacement output file. The loads and displacement output file contains the computed applied body forces, resultant forces and moments, and the centroidal displacements and twist. Table 13 of Section 7 explains how to interpret the data in the loads and displacements output file.
PANEL_FILE	A logical switch. Setting PANEL_FILE to <i>true</i> tells Co-Blade to generate the panel data output file. The panel data output file contains information regarding the effective material properties of the panel laminates, and the effective beam normal stresses, shear stresses, and panel buckling criteria. Table 14 of Section 7 explains how to interpret the data in the panel data output file.
LAMINA_FILE	A logical switch. Setting LAMINA_FILE to <i>true</i> tells Co-Blade to generate the lamina data output file. The lamina data output file contains information regarding the strains, stresses, and maximum stress failure criteria within each individual lamina of the entire blade, in addition to the effective material properties of the panel laminates and panel buckling criteria. Table 15 of Section 7 explains how to interpret the data in the lamina data output file.
DATA_GUI	A logical switch. Setting DATA_GUI to <i>true</i> opens a graphical user interface (GUI) to visualize blade geometry, panel, and layer data. This GUI plots a 3D representation of the blade and allows the user to select via a spreadsheet which panels and/or laminas are shown in the plot. Also, the user can select which output parameter (e.g. Effective modulus, panel thickness, strain, stress, etc.) are visualized in the selected panels and/or laminas. An example of this GUI is shown in Figures A-1 and A-2, with further explanation on how to use the GUI in the figure captions.
SAVE_PLOTS	A logical switch. Setting SAVE_PLOTS to <i>true</i> causes any figure that is created by the PLOT_* flags (below) to be saved to a file. The format of the image file is set by the SAVE FIG_FMT flag.
SAVE FIG_FMT	SAVE FIG_FMT is used to set the format of the saved image files. Enter -fig to save the images as MATLAB .fig files (recommended), otherwise a comma delimited (no spaces) list of format options can be used to save the images as a variety of bitmap or vector formats. When saving image files, Co-Blade calls the <i>export_fig()</i> function created by Oliver Woodford to create publication quality figures. For detailed explanation on how to call the <i>export_fig()</i> function, please refer to the following link for full documentation:

	<p><a href="http://www.mathworks.com/matlabcentral/fileexchange/23629">http://www.mathworks.com/matlabcentral/fileexchange/23629</a></p> <p>For simplicity, a string such as <code>-png,-r200,-a2</code> can be entered, which creates the image files as <code>.png</code> files with 200 DPI resolution and a low level of anti-aliasing (can select <code>-a1</code> for no anti-aliasing and up to <code>-a4</code> for the highest level).</p>
PLOT_OPT_ITER	A logical switch. Setting PLOT_OPT_ITER to <i>true</i> will create Figure 6 and Figure 14 which give information about the progress of the composite layup optimization algorithm (the appearance of Figure 14 may vary depending on which optimization algorithm is selected via OPT_METHOD). Ignored if OPTIMIZE is <i>false</i> .
PLOT_F_BLD	A logical switch. Setting PLOT_F_BLD to <i>true</i> creates a figure showing the external blade shape with arrows indicating the magnitude and direction of the applied aerodynamic forces and body forces (net weight and centrifugal). This figure can be created in view the global or blade reference frame (set by the PLOT_GBL_SYS flag). An example of this figure is shown in Figures A-3 and A-4.
PLOT_DISP_BLD	A logical switch. Setting PLOT_DISP_BLD to <i>true</i> creates a figure showing the blade external geometry and the displaced blade external geometry. This figure can be created in view the global or blade reference frame (set by the PLOT_GBL_SYS flag). An example of this figure is shown in Figures A-3 and A-4.
PLOT_GBL_SYS	A logical switch. Setting PLOT_GBL_SYS to <i>true</i> creates the figure described by PLOT_F_BLD or PLOT_DISP_BLD within view of the global reference frame, setting this to false creates the figure in view of the blade reference frame. An example of this figure is shown in Figures A-3 and A-4.
PLOT_YMOD	A logical switch. Setting PLOT_YMOD to <i>true</i> creates a figure showing the three-dimensional blade geometry with the panel laminates colored by their effective Young's modulus. An example of this figure is shown in Figure A-7.
PLOT_GMOD	A logical switch. Setting PLOT_GMOD to <i>true</i> creates a figure showing the three-dimensional blade geometry with the panel laminates colored by their effective shear modulus. An example of this figure is shown in Figure A-8.
PLOT_MASS_DEN	A logical switch. Setting PLOT_MASS_DEN to <i>true</i> creates a figure showing the span-variant mass density. An example of this figure is shown in Figure A-9.
PLOT_PRIN_ANG	A logical switch. Setting PLOT_PRIN_ANG to <i>true</i> creates a figure showing the span-variant angle between the blade coordinate system x-axis and the flapwise principal axis with respect to the mass center, tension center, and shear center. An example of this figure is shown in Figure A-10.
PLOT_AT_STFF	A logical switch. Setting PLOT_AT_STFF to <i>true</i> creates a figure showing the span-variant axial stiffness and torsional stiffness. An example of this figure is shown in Figure A-11.
PLOT_BSTFF	A logical switch. Setting PLOT_BSTFF to <i>true</i> creates a figure showing the span-variant flapwise and edgewise effective bending stiffnesses with respect to the mass center, tension center, and shear center principal axes, as well as the effective bending stiffnesses with respect to the x-y axes of the blade coordinate system. An example of this figure is shown in Figure A-12.
PLOT_INER	A logical switch. Setting PLOT_INER to <i>true</i> creates a figure showing the span-variant flapwise and edgewise mass moments of inertia per unit length with respect to the mass center, tension center, and shear center principal axes, as well as the mass moments of inertia per unit length with respect to the x-y axes of the blade coordinate system. An example of this figure is shown in Figure A-13.
PLOT_CENTERS	A logical switch. Setting PLOT_CENTERS to <i>true</i> creates a figure showing the span-variant locations of the mass centers, tension centers, and shear centers with respect to the x-y coordinates of the blade reference coordinate systems, as well as normalized chordwise offsets. An example of this figure is shown in Figure A-14.
PLOT_NORMS	A logical switch. Setting PLOT_NORMS to <i>true</i> creates a figure showing the three-dimensional blade geometry with the panel laminates colored by their effective beam axial stress, $\sigma_{zz}$ . An example of this figure is shown in Figure A-15.

PLOT_SHEARS	A logical switch. Setting PLOT_SHEARS to <i>true</i> creates a figure showing the three-dimensional blade geometry with the panel laminates colored by their effective beam shear stress, $\tau_{zs}$ . An example of this figure is shown in Figure A-16.
PLOT_BCRIT	A logical switch. Setting PLOT_BCRIT to <i>true</i> creates a figure showing the three-dimensional blade geometry with the panel laminates colored by their panel buckling criteria. A buckling criteria, R, greater than 1 indicates that the panel has buckled under the combined effect of compression and shear, while a value of R less than 1 indicates that the panel has not buckled. An example of this figure is shown in Figure A-17.
PLOT_E11	A logical switch. Setting PLOT_E11 to <i>true</i> creates a figure of the span variant and chordwise variant normal strains in direction 1 (the principal direction), $\varepsilon_{11}$ , within each individual lamina of the top, bottom, and shear web surfaces. An example of this figure is shown in Figure A-18.
PLOT_E22	A logical switch. Setting PLOT_E22 to <i>true</i> creates a figure of the span variant and chordwise variant normal strains in direction 2 (the lateral direction), $\varepsilon_{22}$ , within each individual lamina of the top, bottom, and shear web surfaces. A figure similar to this is shown in Figure A-18.
PLOT_E12	A logical switch. Setting PLOT_E12 to <i>true</i> creates a figure of the span variant and chordwise variant principal shear strains, $\gamma_{12}$ , within each individual lamina of the top, bottom, and shear web surfaces. A figure similar to this is shown in Figure A-18.
PLOT_S11	A logical switch. Setting PLOT_S11 to <i>true</i> creates a figure of the span variant and chordwise variant normal stresses in direction 1 (the principal direction), $\sigma_{11}$ , within each individual lamina of the top, bottom, and shear web surfaces. An example of this figure is shown in Figure A-19.
PLOT_S22	A logical switch. Setting PLOT_S22 to <i>true</i> creates a figure of the span variant and chordwise variant normal stresses in direction 2 (the lateral direction), $\sigma_{22}$ , within each individual lamina of the top, bottom, and shear web surfaces. A figure similar to this is shown in Figure A-19.
PLOT_S12	A logical switch. Setting PLOT_S12 to <i>true</i> creates a figure of the span variant and chordwise variant principal shear stresses, $\tau_{12}$ , within each individual lamina of the top, bottom, and shear web surfaces. A figure similar to this is shown in Figure A-19.
PLOT_S11_FC	A logical switch. Setting PLOT_S11_FC to <i>true</i> creates two figures showing the span variant and chordwise variant failure criteria in compression and tension for the normal stresses in direction 1 (the principal direction) within each individual lamina of the top, bottom, and shear web surfaces. Examples of these figures are shown in Figures A-20 and A-21.
PLOT_S22_FC	A logical switch. Setting PLOT_S22_FC to <i>true</i> creates two figures showing the span variant and chordwise variant yielding criteria in compression and tension for the normal stresses in direction 2 (the lateral direction) within each individual lamina of the top, bottom, and shear web surfaces. Examples of figures similar to these are shown in Figures A-20 and A-21.
PLOT_S12_FC	A logical switch. Setting PLOT_S12_FC to <i>true</i> creates a figure showing the span variant and chordwise variant yielding criteria for the principal shear stresses within each individual lamina of the top, bottom, and shear web surfaces. An example of this figure is shown in Figure A-22.
PLOT_MODE_D	A logical switch. Setting PLOT_MODE_D to <i>true</i> creates three figures showing the span variant flapwise and edgewise modal displacements, and the modal twist for each mode calculated by the BModes code. The first of these figures shows the component of modal displacement normal to the reference plane of rotation (denoted as flapwise modal displacement), and the second of these figures shows the projection of modal displacement in the reference plane of rotation (denoted as edgewise or lag modal displacement). A third figure is also created showing the span variant modal twist, which for practical purposes and for modal-based codes such as FAST may be defined as the projection of section twist in a plane that is normal to both the reference plane of rotation and the blade reference axis (usually the pitch axis) [2]. An example of such figures is shown in Figure A-23.
PLOT_MODE_S	A logical switch. Setting PLOT_MODE_S to <i>true</i> creates two figures showing the span variant flapwise and edgewise modal slopes for each mode calculated by the BModes code. The first of these figures shows the slope of modal displacement curve projected onto a plane that passes through

	the undeformed blade reference axis (the pitch axis) and is normal to the reference plane of rotation (denoted as flapwise modal slope). The second of these figures shows the slope of modal displacement curve projected in the reference plane of rotation (denoted as edgewise or lag model slope). A figure similar to this is shown in Figure A-23.
PLOT_APPLOADS	A logical switch. Setting PLOT_APPLOADS to <i>true</i> creates a figure of the span variant x-y-z components of the aerodynamic forces and moments and body forces (net weight and centrifugal) with respect to the blade coordinate system. An example of this figure is shown in Figure A-5.
PLOT_RESLOADS	A logical switch. Setting PLOT_RESLOADS to <i>true</i> creates a figure of the span variant x-y-z components of the resultant shear forces and bending moments with respect to the blade coordinate system, resulting from the applied aerodynamic and body loads. An example of this figure is shown in Figure A-6.
PLOT_DEFLECT	A logical switch. Setting PLOT_DEFLECT to <i>true</i> creates a figure showing the span variant displacements and twist angle about the centroidal (tension center) axis, with respect to the blade coordinate system. An example of this figure is shown in Figure A-24.

### 5.3. Airfoil Shape Input File

The number of airfoil shape input files must be equal to or less than the number of blade stations (NUM\_SEC) specified in the main input file. Blade stations with the same airfoil shape, although with possibly different chord lengths, can be described by a single airfoil input file because the airfoil shapes are defined with respect to chord normalized coordinates. The airfoil shape input files can have any name, but must be located in the `\Airfoil_Data` directory. The data format in the airfoil shape input files is identical to that established by the PreComp code [4], which makes these input files directly compatible between the PreComp and Co-Blade codes. The input parameters within the airfoil shape input files are described in Table 8, and the coordinates entered in these files must follow these rules:

1. The leading edge must have coordinates (0,0) and the trailing edge should have coordinates (1,0).
2. The x-coordinates of the airfoil nodes must monotonically increase along the upper surface from the leading edge toward the trailing edge, and then monotonically decrease along the bottom surface from the trailing edge toward the leading edge.
3. The airfoil coordinates along the top and bottom surfaces (separated by the leading and trailing edges) cannot cross each other and must be defined as single valued functions. An example of permissible airfoil shapes is shown in Figure 4. A blunt trailing edge is permissible.

Table 8. Airfoil Shape Input File Parameters

Parameter	Description
<i>N_af_nodes</i>	A positive integer. Number of nodes that describe the airfoil shape. The node ordering begins at the leading edge (0,0), moves over the top surface, reaches the trailing edge (1,0), moves over the lower surface, and terminates at the last node just below the leading edge. An example of this nodal ordering is shown in Figure 11.
<i>Xnode</i>	This column of data defines the x-coordinate of the airfoil shape with respect to the airfoil reference axes. These airfoil reference axes originate at the leading edge, with the positive x-axis directed along the chord line. This coordinate is normalized by the chord length, so its maximum permissible value is 1.
<i>Ynode</i>	This column of data defines the y-coordinate of the airfoil shape with respect to the airfoil reference axes. This coordinate is normalized by the chord length.

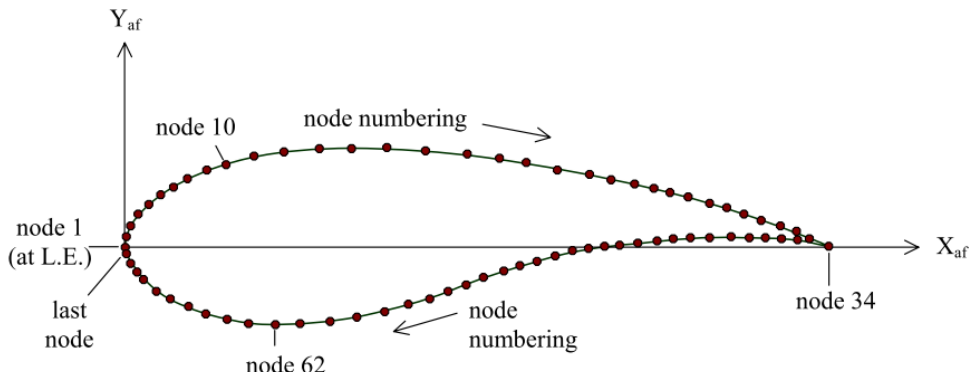


Figure 11. Illustration of how to order the airfoil coordinates. Image reproduced from [4].

## 5.4. Laminate Input File

As shown in the example of Figure 2, the internal composite layup is defined with three components: the top surface, bottom surface, and shear webs. The top and bottom surfaces are defined as the upper and lower parts, respectively, of the section periphery between the leading and trailing edges. The top and bottom surfaces can be divided into an arbitrary number of sectors (or also called “panels”). A sector is a laminate, i.e., a stack of laminas of different composite materials and principal fiber directions, and each lamina is composed of similar plies. The example in Figure 2 shows three sectors on the top and bottom surfaces, where the top middle sector is composed of eight laminas (view AA) and the shear web is composed of five laminas (view BB). However, Co-Blade allows for an arbitrary number of sectors to be defined on the top and bottom surfaces, and for an arbitrary number of laminas/plies within the top, bottom, and web laminates.

The blade’s external shape is completely defined by the airfoil shape input files along with the main input file, and the laminate input files specify the composite layup within the external shape. If multiple blade cross sections have similar structural layups, a single laminate input file may be used to define multiple sections. The laminate input files can have any name, but must be located in the `\Laminate_Data` directory. Also, the data format in the laminate input files is identical to that established by the PreComp code [4], which makes these input files directly compatible between the PreComp and Co-Blade codes. An example of laminate input file is given in Figure 12 below. The length of data in the laminate input files may differ from section to section, but the format and sequence of comments, blank lines, and data blocks stays the same. The laminate data is entered in a hierarchical fashion: first for the top surface, next for the bottom surface, and finally for the webs. Figure 12 shows an example laminate input file with three sectors on the top surface. First the number of sectors on the top surface is entered, and then the x-coordinates (normalized by the chord length) of the points that define the sector boundaries are entered. Next, the lamina-level data is entered for each sector, starting with sector 1. For each sector, we enter number of laminas in each sector, number of plies in each lamina, thickness of each ply in the lamina, principal fiber direction of each lamina, and constituent properties of each ply. In this example, three laminas exist in the first sector of the top surface, so the lamina-level data must be entered on three lines. The lamina numbering proceeds from the exterior surface to the blade interior, with the first lamina at the exterior surface. Similar information is then entered for the bottom surface and finally for the webs. The data entry is self-explanatory in the example laminate files, but you may refer to Table 9 for a detailed description of the input parameters.

```

Composite laminae lay-up inside the blade section
*****
***** TOP SURFACE *****
3      N_scts(1): no of sectors on top surface

normalized chord location of nodes defining airfoil sectors boundaries (xsec_node)
0.0      0.15      0.50      1.00
.....
Sect_num      no of laminae (N_laminas)
1            3

lamina      num of thickness   fibers_direction  composite_material ID
number      plies      of ply (m)      (deg)          (-)
lam_num     N_plies    Tply        Thth_lam       Mat_id
1           1          0.000381      0              3 (gelcoat)
2           1          0.00051       0              4 (nexus)
3           33         0.00053       20             2 (double-bias)
.....
Sect_num      no of laminae
2            7

lamina      num of thickness   fibers_direction  composite_material ID
number      plies      of ply (m)      (deg)          (-)
lam_num     N_plies    Tply        Thth_lam       Mat_id
1           1          0.000381      0              3 (gelcoat)
2           1          0.00051       0              4 (nexus)
3           17         0.00053       20             2 (double-bias)
4           38         0.00053       30             1 (uni)
5           0          0.003125      0              5 (balsa)
6           37         0.00053       30             1 (uni)
7           16         0.00053       20             2 (double-bias)
.....
Sect_num      no of laminae
3            5

lamina      num of thickness   fibers_direction  composite_material ID
number      plies      of ply (m)      (deg)          (-)
lam_num     N_plies    Tply        Thth_lam       Mat_id
1           1          0.000381      0              3 (gelcoat)
2           1          0.00051       0              4 (nexus)

```

Figure 12. Example of a laminate input file (continued to the next page). Reproduced from [4].

```

3      17  0.00053    20      2 (double-bias)
4      38  0.00053    30      1 (uni)
5       0  0.003125   0       5 (balsa)
6      37  0.00053    30      1 (uni)
7      16  0.00053    20      2 (double-bias)
.....  

Sect_num  no of laminae  

3          5  

lamina  num of thickness  fibers_direction  composite_material ID  

number  plies  of ply (m)  (deg)           (-)  

lam_num N_plies   Tply     Tht_lam        Mat_id  

1       1  0.000381    0      3 (gelcoat)  

2       1  0.00051     0      4 (nexus)  

3      17  0.00053    20     2 (double-bias)  

4       0  0.003125   0      5 (balsa)  

5      16  0.00053    0      2 (double-bias)  

***** BOTTOM SURFACE *****  

3      N_scts(2):  no of sectors on bottom surfaces  

normalized chord location of surface nodes defining sector boundaries (xsec_node)  

0.0      0.15      0.50      1.00  

.....  

Sect_num  no of laminae  

1          3  

lamina  num of thickness  fibers_direction  composite_material ID  

number  plies  of ply (m)  (deg)           (-)  

lam_num N_plies   Tply     Tht_lam        Mat_id  

1       1  0.000381    0      3 (gelcoat)  

2       1  0.00051     0      4 (nexus)  

3      33  0.00053    20     2 (double-bias)  

.....  

Sect_num  no of laminae  

2          7  

lamina  num of thickness  fibers_direction  composite_material ID  

number  plies  of ply (m)  (deg)           (-)  

lam_num N_plies   Tply     Tht_Lam      Mat_Id  

1       1  0.000381    0      3 (gelcoat)  

2       1  0.00051     0      4 (nexus)  

3      17  0.00053    20     2 (double-bias)  

4      38  0.00053    30     1 (uni)  

5       0  0.003125   0      5 (balsa)  

6      37  0.00053    30     1 (uni)  

7      16  0.00053    20     2 (double-bias)  

.....  

Sect_num  no of laminae  

3          5  

lamina  num of thickness  fibers_direction  composite_material ID  

number  plies  of ply (m)  (deg)           (-)  

lam_num N_Plies  Tply     Tht_Lam      Mat_Id  

1       1  0.000381    0      3 (gelcoat)  

2       1  0.00051     0      4 (nexus)  

3      17  0.00053    20     2 (double-bias)  

4       0  0.003125   0      5 (balsa)  

5      16  0.00053    0      2 (double-bias)  

***** WEBS *****  

Laminae schedule for webs (input required only if webs exist at this section):  

web_num  no of laminae (N_weblam)  

1          3  

lamina  num of thickness  fibers_direction  composite_material ID  

number  plies  of ply (m)  (deg)           (-)  

wlam_num N_plies  w_tply   Tht_Wlam     Wmat_Id  

1       38  0.00053     0      1 (uni)  

2       0  0.003125   0      5 (balsa)  

3      37  0.00053     0      1 (uni)  

.....  

web_num  no of laminae  

2          3  

lamina  num of thickness  fibers_direction  composite_material ID  

number  plies  of ply (m)  (deg)           (-)  

wlam_num N_plies  w_tply   Tht_Wlam     Wmat_Id  

1       38  0.00053     0      1 (uni)  

2       0  0.003125   0      5 (balsa)  

3      37  0.00053     0      1 (uni)

```

Figure 12. Example of a laminate input file (continued from previous page). Reproduced from [4].

Table 9. Laminate Input File Parameters

Parameter	Description
N_scts	A positive integer. The number of sectors on the surface periphery. N_scts(1) and N_scts(2) are the number of sectors on the top and bottom surfaces, respectively.
xsec_node	This sequence of values specifies the x-coordinates of the sector boundaries on the top and bottom surfaces. This x-coordinate is normalized with respect to the chord length and is referenced to the airfoil coordinate frame (Figure 11). In the example of Figure 12, we have three sectors on the top surface, which imply four points that define the sector boundaries. The x-coordinates of these four points are 0, 0.15, 0.50, and 1.0. Sector 1 is bounded by x-coordinates 0 and 0.15, sector 2 is bounded by x-coordinates 0.15 and 0.5, and sector 3 is bounded between x-coordinates 0.50 and 1.0. The x-coordinates of sector boundaries must be positive and in ascending order. The first and last x-coordinates must be equal to 0 and 1, representing the leading and trailing edges, respectively.
Sect_num	A positive integer. The sector identification number, the first sector has value 1.
N_laminas	A positive integer. Number of laminas for a particular sector identified in the file.
lam_num	Lamina identification number, a positive integer. The first lamina is always at the exterior surface of the blade and the numbering proceeds from the exterior to the interior of the blade.
N_plies	A positive integer. The number of plies in the identified lamina.
Tply	The thickness of each ply in the identified lamina. Units [m].
Tht_lam	Ply angle representing the orientation of the principal fiber direction in the identified lamina. Figure 1 shows how a positive ply angle is defined, where S is a point on the blade surface at which we wish to determine the ply angle. The r-t-s is a right-hand coordinate system with r axis parallel to the blade axis and pointing outboard. The t axis is normal to r and tangent to the blade surface. The n axis is normal to the blade surface at point S. Line SL is the principal material direction (longitudinal, or direction-1) and $\alpha$ , the angle between SL and r axis, represents the ply angle. A rotation $\alpha$ of the r-t-s axes system about the n axis thus aligns the r axis with principal material direction SL. A positive rotation about the n axis implies a positive ply angle. Units [deg].
Mat_id	Material identification number, this number assigns a set of constitutive material properties to the plies specified in the lamina. This material identification number corresponds to the materials in the materials input file, described in the following section.
web_num	The web identification number, same as webNum defined in the main input file.
N_weblams	A positive integer. Number of laminas in the identified web. Unlike the top and bottom surfaces, which may have multiple laminates (sector, panels, or stacks of laminas), a web is assumed to have only a single laminate. Most blades are built this way.
W_tply	The thickness of each ply in the identified web. Note: if webs exist at this current cross section, there should always be NUM_WEBS number of laminate tables to read, even if there are less than NUM_WEBS number of webs currently defined at the blade station. If one or more of the webs are not defined at the blade station enter 0 for their number of laminas (N_laminas). See the example files provided in <i>WindTurbineRef.inp</i> for further clarification. This convention is used to keep compatibility with the PreComp [4] code for the laminate input files. Units [m].
Tht_Wlam	The ply angle representing the orientation of the principal fiber direction of each ply in the identified web. Note, the definition of ply angle for a web lamina follows that of Tht_lam defined earlier. However, for the webs the n axis, normal to the web surface, always points toward the leading edge. Units [deg].

## 5.5. Materials Input File

The materials input file contains the constitutive properties and ultimate strengths which are assigned to the laminas in the laminate input files. The parameters within the material input file are described in Table 10. The materials input file can have any name, but should be placed in the `\Material_Data` directory. When Co-Blade is run in analysis mode any number of materials can be entered in the materials input file. However, when Co-Blade is run in optimization mode (`OPTIMIZE = true`) it expects to read only 8 materials from this file, as shown in the example material input file of Figure 13. The 8 materials must be listed in the order of the `matName` column, where the material names in the `matName` column correspond to the materials described in Section 3.2.

Table 10. Materials Input File Parameters

Parameter	Description
<code>Mat_id</code>	A positive integer. Material identification number.
<code>E11</code>	Young's modulus in the principal direction and assumed to be the same in tension and compression. Units [Pa].
<code>E22</code>	Young's modulus in the lateral direction (normal to the principal direction) and assumed to be the same in tension and compression. Units [Pa].
<code>G12</code>	Shear modulus with respect to the principal and lateral directions. Units [Pa].
<code>nu12</code>	Poisson's ratio, defined as the contraction strain in direction 2 (lateral direction) caused by unit extensional strain in direction 1 (principal direction). $\nu_{12}$ is one of the Poisson's ratios, which is related to $\nu_{21}$ as follows: $\nu_{21} = \nu_{12} \sqrt{\frac{E_{22}}{E_{11}}}$
<code>density</code>	Density of the material. Units [ $\text{kg}/\text{m}^3$ ].
<code>s11_ft</code>	Tensile stress at which failure occurs in direction 1 (the principal direction). A positive quantity. Can also enter <code>Inf</code> if this quantity is unknown. Units [Pa].
<code>s11_fc</code>	Compressive stress at which failure occurs in direction 1 (the principal direction). A negative quantity. Can also enter <code>-Inf</code> if this quantity is unknown. Units [Pa].
<code>s22_yT</code>	Tensile stress at which yielding occurs in direction 2 (the lateral direction). A positive quantity. Can also enter <code>Inf</code> if this quantity is unknown. Units [Pa].
<code>s22_yc</code>	Compressive stress at which yielding occurs in direction 2 (the lateral direction). A negative quantity. Can also enter <code>-Inf</code> if this quantity is unknown. Units [Pa].
<code>s12_y</code>	Shear stress at which yielding occurs within the plane of directions 1-2. Can also enter <code>Inf</code> if this quantity is unknown. A positive quantity. Units [Pa].
<code>matName</code>	This is the material name associated with the material identifier. Any name can be defined for this parameter but the name cannot contain spaces.

Material input file. When <code>OPTIMIZE=true</code> 8 materials are listed in order of the <code>matName</code> column.											
matID	E11	E22	G12	nu12	density	s11_ft	s11_fc	s22_yT	s22_yc	s12_y	matName
(-)	(Pa)	(Pa)	(Pa)	(-)	( $\text{kg}/\text{m}^3$ )	(Pa)	(Pa)	(Pa)	(Pa)	(-)	
1	14e9	13e9	12e9	0.51	1780	144e6	-213e6	Inf	-Inf	30e6	(blade-root)
2	22e9	27e9	16e9	0.30	1870	377e6	-411e6	40e6	-141e6	53e6	(blade-shell)
3	36e9	11e9	3e9	0.32	1800	711e6	-1200e6	38e6	-183e6	66e6	(spar-uni)
4	61e6	60e6	19e6	0.20	120	2.6e6	-1.4e6	2.5e6	-1.4e6	7e5	(spar-core)
5	61e6	60e6	19e6	0.20	120	2.6e6	-1.4e6	2.5e6	-1.4e6	7e5	(LEP-core)
6	61e6	60e6	19e6	0.20	120	2.6e6	-1.4e6	2.5e6	-1.4e6	7e5	(TEP-core)
7	22e9	27e9	16e9	0.30	1870	377e6	-411e6	40e6	-141e6	53e6	(web-shell)
8	61e6	60e6	19e6	0.20	120	2.6e6	-1.4e6	2.5e6	-1.4e6	7e5	(web-core)

Figure 13. Example of a material input file when Co-Blade is run in optimization mode.

## 5.6. Optimization Input Files

The file specified by `INITX_FILE` allows you to enter preliminary values for the design variables, and the parameters in this file are described in Table 11—see the example files provided in the `\Optimization_Data` folder to see how to format this type of input file. The `PatternSearchOptions.inp`, `GradientSearchOptions.inp`, and `ParticleSwarmOptions.inp` files in the `\Optimization_Data` folder contain parameters that control the behavior of the Pattern Search, Gradient Search, and Particle Swarm optimization algorithms, respectively, which are used to optimize the blade composite layup. A full description of the parameters controlling each optimization algorithm is beyond the scope of this user’s guide, but a brief description can be seen in the example input files and full documentation can be found at:

- Pattern Search Optimization: <http://www.mathworks.com/help/toolbox/gads/bq54rjg.html>
- Gradient Search Optimization: <http://www.mathworks.com/help/toolbox/optim/ug/fmincon.html>
- Particle Swarm Optimization: <http://www.mathworks.com/matlabcentral/fileexchange/25986>

Table 11. Optimization Design Variables

Parameter	Description
<code>w_cap_inb</code> , <code>w_cap_oub</code>	width of the spar cap normalized by the chord length at the <code>INB_STN</code> and <code>OUN_STN</code> blade stations, respectively.
<code>t_blade_root</code>	thickness of the “blade-root” material at the <code>INB_STN</code> blade station.
<code>t_blade_skin1</code> ... <code>t_blade_skinN</code>	thickness of “blade-shell” material at control points 1 through <code>NUM_CP</code> . The control points are equally spaced along the blade between the <code>TRAN_STN</code> and <code>OUN_STN</code> blade stations.
<code>t_cap_uni1</code> ... <code>t_cap_uniN</code>	thickness of “spar-uni” material at control points 1 through <code>NUM_CP</code> . The control points are equally spaced along the blade between the <code>TRAN_STN</code> and <code>OUN_STN</code> blade stations.
<code>t_cap_core1</code> ... <code>t_cap_coreN</code>	thickness of “spar-core” material at control points 1 through <code>NUM_CP</code> . The control points are equally spaced along the blade between the <code>TRAN_STN</code> and <code>OUN_STN</code> blade stations.
<code>t_lep_core1</code> ... <code>t_lep_coreN</code>	thickness of “LEP-core” material at control points 1 through <code>NUM_CP</code> . The control points are equally spaced along the blade between the <code>TRAN_STN</code> and <code>OUN_STN</code> blade stations.
<code>t_tep_core1</code> ... <code>t_tep_coreN</code>	thickness of “TEP-core” material at control points 1 through <code>NUM_CP</code> . The control points are equally spaced along the blade between the <code>TRAN_STN</code> and <code>OUN_STN</code> blade stations.
<code>t_web_skin1</code> , <code>t_web_skin2</code>	thickness of “web-shell” material at the two control points located at <code>INB_STN</code> and <code>OUN_STN</code> .
<code>t_web_core1</code> , <code>t_web_core2</code>	thickness of “web-core” material at the two control points located at <code>INB_STN</code> and <code>OUN_STN</code> .

\*Note: the thickness  $t$  entered into the `INITX_FILE` input file is the material thickness in  $\frac{1}{2}$  of the symmetric laminate—multiplying this value by 2 obtains the total thickness in the laminate.

## 6. Executing Co-Blade

First, follow the guidelines in Sections 5 to create the main input file, the airfoil shape files, the laminate files, and the materials input file. Read through the sample files provided with Co-Blade and modify them to suit your composite blade. Note that all auxiliary input files are identified within the main input file. If running Co-Blade in optimization mode, you may wish to also modify the `INITX_FILE` and optimization algorithm input files.

The present working directory should include the Co-Blade executable, the BModes executable, `Active_Input_Files.inp`, and main input file. The airfoil shape files should reside in a directory named `\Airfoil_Data`, the laminate files should reside in a directory named `\Laminate_Data`, the material files should reside in the directory named `\Material_Data`, and the file specified by `INITX_FILE` and the optimization algorithm input files should reside in the `\Optimization_Data` folder—all four of these directories reside within the present working directory. Next, open the text file named `Active_Input_Files.inp`, included with Co-Blade, and write the name of the main input file on the first line of this text file. If you have multiple composite blade models and you wish to perform a batch analysis, you can list the name of each main input file on multiple rows of the file `Active_Input_Files.inp`.

Co-Blade must be run from the operating system's command prompt. Windows Vista/7 users can access the command prompt by clicking Start, typing "cmd", and pressing enter. In older versions of Windows the user will need to click Start, and then click Run before typing the "cmd" command. Once in the command prompt, change to the directory where the compiled Co-Blade executable and all input files reside. Finally, issue the command `CoBlade` at the command prompt. Co-Blade will then read the names of the input files listed in `Active_Input_Files.inp` and perform a sequential analysis for each file and create the corresponding output data files for each analysis.

Notes about runtime performance: Co-Blade typically completes an entire analysis within a matter of seconds or less; however, creation of the figures requires additional time. If speed is essential, it is recommended to disable the automatic creation of figures to maximize performance. Also, the compiled version of Co-Blade can run significantly slower compared to executing Co-Blade directly within MATLAB (unfortunately). This is because the MATLAB MCR must be unpacked by the operating system each time the compiled version of CoBlade is executed. Unpacking of the MCR can take anywhere from 10-45 seconds, while execution of a single CoBlade analysis case takes only a few seconds.

### 6.1. Error Messages and Warning

Co-Blade will perform extensive checks to ensure that the user supplied data is within range, consistent, and realizable. Detected errors will be displayed within the command prompt and Co-Blade will give a self-explanatory message on how to correct the error. If you experience trouble creating a new Co-Blade model, please carefully review the sample files provided with Co-Blade and modify them only a few (or less) lines at a time until they suit your composite blade model.

### 6.2. Analysis Mode

When both `OPTIMIZE` and `OPT_PITAXIS` are set to *false* Co-Blade runs in analysis mode. In analysis mode Co-Blade will read the laminate input files (described in Section 5.4) to define the internal structural layup of the blade. In analysis mode the structural properties and complete structural analysis are computed within a few seconds or less, and if any output figures have been requested they will be immediately created.

### 6.3. Optimization Mode

If either `OPTIMIZE` or `OPT_PITAXIS` are set to *true* Co-Blade runs in optimization mode. After Co-Blade finishes running in optimization mode, a special output file with the suffix `*_OPT.inp` will be created, which is just an exact copy of the main input file except that any parameters that have been overwritten by the optimization algorithms will be written in this new file—such parameters that are ignored and then are overwritten during optimization are: `pitAxis`, `int_str_file`, `webNum`, `inbStn`, `oubStn`, `inbChLoc`, and `oubChLoc`.

When `OPTIMIZE` is set to *true*, Co-Blade defines the internal structural layup of the blade according to Section 3.2 (rather than by reading the laminate input files) and will optimize this layup of composite materials using the optimization algorithm selected by `OPT_METHOD`. For a given external blade shape and design load, Co-Blade will vary the placement and thickness of the composite materials as described in Section 3.2 in order to minimize the fitness function  $f(\vec{x})$ , which minimizes the blade mass while satisfying constraints on maximum stress, buckling, tip deflection, and separation of the blade natural frequencies from the blade rotation frequency. Mathematically, this optimization problem is formulated as:

minimize:  $f(\vec{x}) = \text{BladeMass} * \prod_{n=1}^8 \max\{1, p_n\}^2$

$$p_1 = \frac{\sigma_{11,max}}{\sigma_{11,fT}}$$

$$p_2 = \frac{\sigma_{11,min}}{\sigma_{11,fc}}$$

$$p_3 = \frac{\sigma_{22,max}}{\sigma_{22,yT}}$$

$$p_4 = \frac{\sigma_{22,min}}{\sigma_{22,yc}}$$

$$p_5 = \frac{|\tau_{12}|_{,max}}{\tau_{12,y}}$$

$$p_6 = \left( \frac{\sigma}{\sigma_{buckle}} \right)^\alpha + \left( \frac{\tau}{\tau_{buckle}} \right)^\beta$$

$$p_7 = \frac{\text{tipDeflect}}{\text{MAX\_TIP\_D}}$$

$$p_8 = \max\left\{ \frac{\text{MIN\_FREQ\_SEP}}{|\omega_m - \omega_{rotor}|} \right\}, m = 1, \dots M_{modes}$$

subject to:  $\overrightarrow{x_{LB}} \leq \vec{x} \leq \overrightarrow{x_{UB}}$

$$A\vec{x} \leq \bar{b}$$

where  $\vec{x}$  is the vector of design variables described in Table 11. The fitness function  $f(\vec{x})$  is minimized when the blade mass is minimal and all of the penalty factors,  $p_1-p_8$ , are less than 1. Penalty factors  $p_1-p_5$  are greater than 1 if the computed lamina-level stresses exceed the materials' maximum allowable stresses which were entered in the materials input file. Penalty factor  $p_6$  is greater than 1 if a panel (i.e. laminate) has buckled under the combined effects of compression and shear (see [10, 11] or comments in the Co-Blade source code for further theory on how critical buckling stresses  $\sigma_{buckle}$  and  $\tau_{buckle}$  are computed—the exponents  $\alpha$  and  $\beta$  are determined from the boundary conditions of the panel). Penalty factor  $p_7$  is greater than 1 if the maximum allowable tip deflection (MAX\_TIP\_D) has been exceeded. Penalty factor  $p_8$  is greater than 1 if the difference between the blade natural frequency and the rotor rotation frequency is less than MIN\_FREQ\_SEP. In order to produce feasible geometry, the design variables are also subject to lower and upper bounds ( $\overrightarrow{x_{LB}}$  and  $\overrightarrow{x_{UB}}$ ) and linear inequality constraints ( $A\vec{x} \leq \bar{b}$ ).

During optimization of the composite layup, if PLOT\_OPT\_ITER is set *true* than Figure 6 and Figure 14 will be created which give information on the current state of the design variables and progress of the optimization algorithm. Figure 14 also contains buttons that can be activated by the user to either prematurely stop, or pause and resume the optimization algorithm.

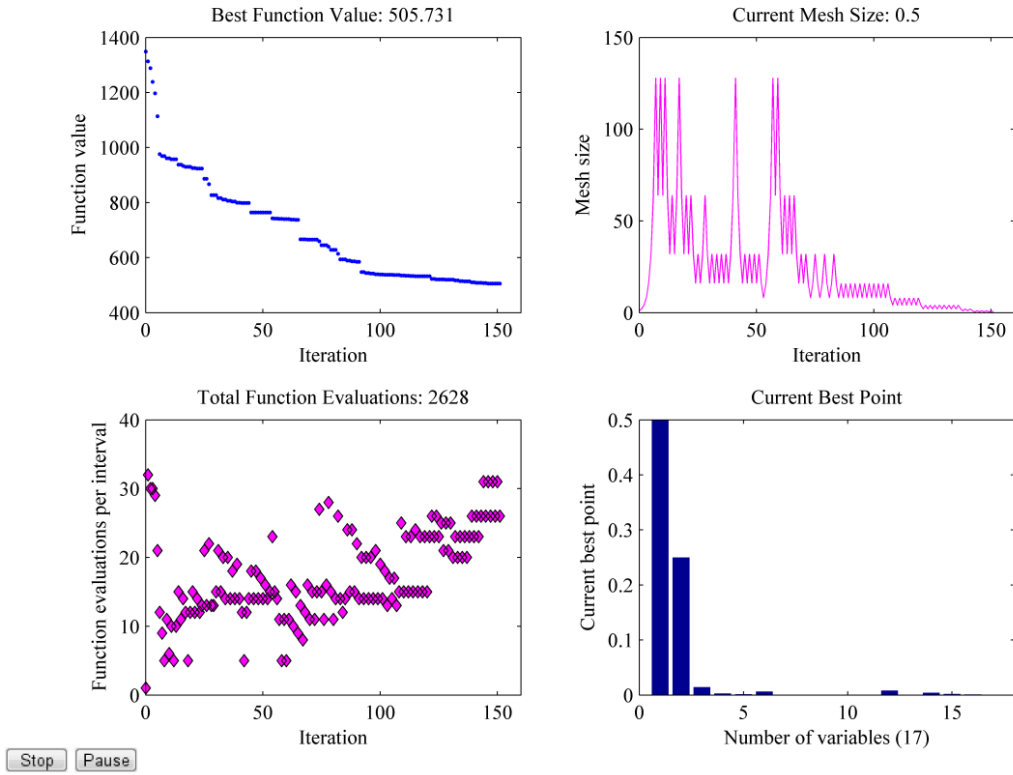


Figure 14. Example of information displayed about the current state of the pattern search optimization algorithm. The information displayed in this figure will vary depending on which optimization algorithm is selected by OPT\_METHOD.

## 7. Output Data Description

Co-Blade creates several text output files which can be viewed with any text editor or imported into any spreadsheet program, such as Excel. The text output files will have the file extension *.out*, and the prefix of the filename is the same as the corresponding main input file, plus an additional suffix that indicates the type of output data within the file. To assist in the post-processing of the output data, Co-Blade can also create a variety of figures for instant visual feedback. Examples of the figures created by Co-Blade are shown in Appendix A and the instructions for how to create each figure were given in Table 7. Note that creating these figures requires additional computational time, so if speed is essential it is recommended to disable the automatic creation of figures.

### 7.1. Structural Properties Data File

The structural properties output file has the suffix *\*\_StrProps.out*, and it contains the computed principal axes orientation, stiffnesses, mass, mass moments of inertia, and centers of mass, tension, and shear. The parameters within this file are given in Table 12.

Table 12. Structural Properties Output File Parameters

Parameter	Description
sec	The blade station, starting with 1 at the blade root.
zSec	z-coordinate measured along the blade pitch axis, starting with 0 at the blade root. Units [m].
aeroTwst	Echo of the value aeroTwst, described in Table 5. Units [deg].
chord	Echo of the value chord, described in Table 5. Units [m].
pitAxis	Echo of the value pitAxis, described in Table 5.
mass_den	Section mass per unit length. Units [kg/m].
iner_tw	Angle between the blade coordinate system x-axis and the section flapwise principal inertial axis. The principal inertial axes are defined as the principal axes w.r.t. the center of mass. A positive angle represents a right handed rotation about the blade pitch axis. See Figure 10. Units [deg].
cent_tw	Angle between the blade coordinate system x-axis and the section flapwise principal centroidal axis. The principal centroidal axes are defined as the principal axes w.r.t. the tension center. See Figure 10. Units [deg].
elas_tw	Angle between the blade coordinate system x-axis and the section flapwise principal elastic axis. The principal elastic axes are defined as the principal axes w.r.t the shear center. See Figure 10. Units [deg].
axial_stff	Axial stiffness. Units [N].
tor_stff	Torsional stiffness. Units [ $N\cdot m^2$ ].
EIx	Bending stiffness about the blade coordinate system x-axis. Units [ $N\cdot m^2$ ].
EIy	Bending stiffness about the blade coordinate system y-axis. Units [ $N\cdot m^2$ ].
EIxy	Cross bending stiffness w.r.t. the blade coordinate system x-y axes. Units [ $N\cdot m^2$ ].
flapEI_cm	Flapwise bending stiffness w.r.t. the section principal inertial axes. Units [ $N\cdot m^2$ ].
edgeEI_cm	Edgewise bending stiffness w.r.t. the section principal inertial axes. Units [ $N\cdot m^2$ ].
flapEI_tc	Flapwise bending stiffness w.r.t. the section principal centroidal axes. Units [ $N\cdot m^2$ ].
edgeEI_tc	Edgewise bending stiffness w.r.t. the section principal centroidal axes. Units [ $N\cdot m^2$ ].
flapEI_sc	Flapwise bending stiffness w.r.t. the section principal elastic axes. Units [ $N\cdot m^2$ ].
edgeEI_sc	Edgewise bending stiffness w.r.t. the section principal elastic axes. Units [ $N\cdot m^2$ ].
mIx	Mass moment of inertia per unit length about the blade coordinate system x-axis. Units [kg-m].
mIy	Mass moment of inertia per unit length about the blade coordinate system y-axis. Units [kg-m].
mIxy	Mass product moment of inertia per unit length w.r.t. the blade coordinate system x-y axes. Units [kg-m].
flapIner_cm	Flapwise mass moment of inertia per unit length w.r.t. the section principal inertial axes. Units [kg-m].
edgeIner_cm	Edgewise mass moment of inertia per unit length w.r.t. the section principal inertial axes. Units [kg-m].
flapIner_tc	Flapwise mass moment of inertia per unit length w.r.t. the section principal centroidal axes. Units [kg-m].
edgeIner_tc	Edgewise mass moment of inertia per unit length w.r.t. the section principal centroidal axes. Units [kg-m].

flapIner_sc	Flapwise mass moment of inertia per unit length w.r.t. the section principal elastic axes. Units [kg-m].
edgeIner_sc	Edgewise mass moment of inertia per unit length w.r.t. the section principal elastic axes. Units [kg-m].
cm_offset	Chordwise offset of the section center of mass, measured along the chord line from the pitch axis and normalized by the chord.
tc_offset	Chordwise offset of the section tension center, measured along the chord line from the pitch axis and normalized by the chord.
sc_offset	Chordwise offset of the section shear center, measured along the chord line from the pitch axis and normalized by the chord.
x_cm	X-coordinate of the center of mass w.r.t. the blade coordinate system x-y axes. Units [m].
y_cm	Y-coordinate of the center of mass w.r.t. the blade coordinate system x-y axes. Units [m].
x_tc	X-coordinate of the tension center w.r.t. the blade coordinate system x-y axes. Units [m].
y_tc	Y-coordinate of the tension center w.r.t. the blade coordinate system x-y axes. Units [m].
x_sc	X-coordinate of the shear center w.r.t. the blade coordinate system x-y axes. Units [m].
y_sc	Y-coordinate of the shear center w.r.t. the blade coordinate system x-y axes. Units [m].

## 7.2. Loads and Displacements Data File

The loads and displacement output file has the suffix *\*.LoadsDisp.out*, and it contains the computed applied body forces, resultant forces and moments, and the centroidal displacements and twist. The parameters within this file are given in Table 13.

Table 13. Loads and Displacements Output File Parameters

Parameter	Description
sec	Same as sec, described in Table 12.
zSec	Same as zSec, described in Table 12.
px_a	Echo of the value px_a, described in Table 5.
py_a	Echo of the value py_a, described in Table 5.
qz_a	Echo of the value qz_a, described in Table 5.
px_w	Force per unit length in the blade coordinate system x-direction due to net-weight. Net-weight is the sum of self-weight and buoyancy forces. Units [N/m].
py_w	Force per unit length in the blade coordinate system y-direction due to net-weight. Units [N/m].
pz_w	Force per unit length in the blade coordinate system z-direction due to net-weight. Units [N/m].
px_c	Force per unit length in the blade coordinate system x-direction due to centrifugal forces. Units [N/m].
py_c	Force per unit length in the blade coordinate system y-direction due to centrifugal forces. Units [N/m].
pz_c	Force per unit length in the blade coordinate system z-direction due to centrifugal forces. Units [N/m].

Vx	Resultant shear force in the blade coordinate system x-direction, resulting from the applied aerodynamic and body loads. Units [N].
Vy	Resultant shear force in the blade coordinate system y-direction, resulting from the applied aerodynamic and body loads. Units [N].
Vz	Resultant shear force in the blade coordinate system z-direction, resulting from the applied aerodynamic and body loads. Units [N].
Mx	Resultant bending moment about the blade coordinate system x-axis, resulting from the applied aerodynamic and body loads. Units [N-m].
My	Resultant bending moment about the blade coordinate system y-axis, resulting from the applied aerodynamic and body loads. Units [N-m].
Mz	Resultant torsional moment about the blade coordinate system z-axis, resulting from the applied aerodynamic and body loads. Units [N-m].
uo	Transverse displacement of the centroidal axis in the blade coordinate system x-direction due to the applied aerodynamic and body loads. If DISP_CF was set to true, then this displacement value has correction factors applied. Units [m].
vo	Transverse displacement of the centroidal axis in the blade coordinate system y-direction due to the applied aerodynamic and body loads. If DISP_CF was set to true, then this displacement value has correction factors applied. Units [m].
wo	Axial displacement of the centroidal axis in the blade coordinate system z-direction due to the applied aerodynamic and body loads. Units [m].
tz	Angle of twist due to the applied aerodynamic and body loads. A positive angle represents a right handed, rigid body rotation about the section shear center. Units [deg].
tipDeflect	The projected displacement of the centroidal axis at the blade tip in the x-direction of the global coordinate system. This value, in most practical cases, would represent the deflection of the blade tip in the direction of the tower. Units [m].

### 7.3. Panel Data File

The panel data output file has the suffix *\*\_Panel.out*, and it contains information regarding the effective material properties of the panel laminates, and the effective beam normal stresses, shear stresses, and panel buckling criteria. The parameters within this file are given in Table 14.

Table 14. Panel Data Output File Parameters

Parameter	Description
sec	Same as sec, described in Table 12.
zSec	Same as zSec, described in Table 12.
nPanelsTop	The total number of panels along the top surface.
nPanelsBot	The total number of panels along the bottom surface.
nWebs	The total number of web panels.
panel	Panel identification number. The panel ordering starts at the leading edge for the top and bottom surfaces, and for webs starts with the web closest to the leading edge.
nNode	The number of analysis nodes in the panel.
nLam	The number of laminas in the panel.
xc_St	This x-coordinate is normalized by the chord and is referenced to the airfoil coordinate frame (Figure 11). It is the x-coordinate along the airfoil periphery that identifies the panel leading edge.

<code>xc_End</code>	This x-coordinate is normalized by the chord and is referenced to the airfoil coordinate frame (Figure 11). It is the x-coordinate along the airfoil periphery that identifies the panel trailing edge. Note: if the panel is actually a web, then $xc_{St} = xc_{End}$ , and it is the x-coordinate of the mid-wall of the web.
<code>b</code>	The arc-length of the panel, measured along the mid-wall of the panel between the coordinates <code>xc_St</code> and <code>xc_End</code> . Units [m].
<code>t</code>	The total thickness of the panel, measured normal to the airfoil periphery. Units [m].
<code>E_eff</code>	The effective Young's modulus of the panel. Units [Pa].
<code>G_eff</code>	The effective shear modulus of the panel. Units [Pa].
<code>nu_eff</code>	The effective Poisson's ratio of the panel.
<code>density</code>	The effective density of the panel. Units [ $\text{kg}/\text{m}^3$ ].
<code>buckleCrit</code>	<p>The buckling criteria of the panel, <math>R</math>. If <math>R &lt; 1</math>, the panel has not buckled. For the top and bottom panels (idealized as curved plates subjected to compression and shear), <math>R</math> is calculated as [10]:</p> $R = \frac{\sigma_{zz}}{\sigma_{zz,critical}} + \left( \frac{\tau_{zs}}{\tau_{zs,critical}} \right)^{1.5}$ <p>For the web panels (idealized as flat plates subjected to bending and shear) <math>R</math> is calculated as [10]:</p> $R = \left( \frac{\sigma_{zz}}{\sigma_{zz,critical}} \right)^2 + \left( \frac{\tau_{zs}}{\tau_{zs,critical}} \right)^2$
<code>s</code>	The panel curvilinear coordinate, measured along the mid-wall of the panel and starting with $s = 0$ at the panel end closest to the leading edge (defined this way for both the top and bottom panels). For the web panels, $s = 0$ is located at the end of the web which connects to the top surface. Units [m].
<code>s_zz_ou</code>	Effective beam normal stress $\sigma_{zz}$ at the outside edge of the panel. Units [Pa].
<code>s_zz_in</code>	Effective beam normal stress $\sigma_{zz}$ at the inside edge of the panel. Units [Pa].
<code>s_zs</code>	Effective beam shear stress $\tau_{zs}$ , which is constant over the wall's thickness. This is the component of shear stress on the blade z-face in the direction of curvilinear coordinate $s$ . Units [Pa].

## 7.4. Lamina Data File

The lamina data output file has the suffix `*_Lamina.out`, and it contains information regarding the strains, stresses, and maximum stress failure criteria within each individual lamina of the entire blade, in addition to the effective material properties of the panel laminates and panel buckling criteria. The parameters within this file are given in Table 15.

Table 15. Lamina Data Output File Parameters

Parameter	Description
<code>sec</code>	Same as <code>sec</code> , described in Table 12.
<code>zSec</code>	Same as <code>zSec</code> , described in Table 12.
<code>nPanelsTop</code>	Same as <code>nPanelsTop</code> , described in Table 14.
<code>nPanelsBot</code>	Same as <code>nPanelsBot</code> , described in Table 14.
<code>nWebs</code>	Same as <code>nWebs</code> , described in Table 14.
<code>panel</code>	Same as <code>panel</code> , described in Table 14.
<code>nNode</code>	Same as <code>nNode</code> , described in Table 14.
<code>nLam</code>	Same as <code>nLam</code> , described in Table 14.
<code>xc_St</code>	Same as <code>xc_St</code> , described in Table 14.
<code>xc_End</code>	Same as <code>xc_End</code> , described in Table 14.
<code>b</code>	Same as <code>b</code> , described in Table 14.
<code>t</code>	Same as <code>t</code> , described in Table 14.
<code>E_eff</code>	Same as <code>E_eff</code> , described in Table 14.
<code>G_eff</code>	Same as <code>G_eff</code> , described in Table 14.
<code>nu_eff</code>	Same as <code>nu_eff</code> , described in Table 14.
<code>density</code>	Same as <code>density</code> , described in Table 14.
<code>buckleCrit</code>	Same as <code>buckleCrit</code> , described in Table 14.
<code>lam_num</code>	Echo of the value <code>lam_num</code> , described in Table 9.
<code>nPlies</code>	Echo of the value <code>N_Plies</code> , number of plies, described in Table 9.
<code>tPly</code>	Echo of the value <code>Tply</code> , ply thickness, described in Table 9.
<code>fibAng</code>	Echo of the value <code>Tht_lam</code> , principal fiber angle, described in Table 9.
<code>matID</code>	Echo of the value <code>Mat_id</code> , material identification, described in Table 9.
<code>matName</code>	Echo of the value <code>matName</code> , material name, described in Table 10.
<code>s</code>	Same as <code>s</code> , described in Table 14.
<code>e11</code>	Lamina strain in direction 1 (principal direction), $\varepsilon_{11}$ . Computed at the lamina interface location which results in the largest absolute value of $\varepsilon_{11}$ . Units [m/m].
<code>e22</code>	Lamina strain in direction 2 (lateral direction), $\varepsilon_{22}$ . Computed at the lamina interface location which results in the largest absolute value of $\varepsilon_{22}$ . Units [m/m].
<code>e12</code>	Lamina principal shear strain w.r.t. directions 1-2, $\gamma_{12}$ . Computed at the lamina interface location which results in the largest absolute value of $\gamma_{12}$ . Units [rad].
<code>s11</code>	Lamina stress in direction 1 (principal direction), $\sigma_{11}$ . Computed at the lamina interface location which results in the largest absolute value of $\sigma_{11}$ . Units [Pa].

s22	Lamina stress in direction 2 (lateral direction), $\sigma_{22}$ . Computed at the lamina interface location which results in the largest absolute value of $\sigma_{22}$ . Units [Pa].
s12	Lamina principal shear stress w.r.t. directions 1-2, $\tau_{12}$ . Computed at the lamina interface location which results in the largest absolute value of $\tau_{12}$ . Units [Pa].
s11_fcT	The direction-1 (principal direction) tensile stress failure criteria, computed as $\frac{\max\{0,\sigma_{11}\}}{\sigma_{11,fc}}$ .
s11_fcc	The direction-1 (principal direction) compressive stress failure criteria, computed as $\frac{\min\{0,\sigma_{11}\}}{\sigma_{11,fc}}$ .
s22_fcT	The direction-2 (lateral direction) tensile stress yielding criteria, computed as $\frac{\max\{0,\sigma_{22}\}}{\sigma_{22,yT}}$ .
s22_fcc	The direction-2 (lateral direction) compressive stress yielding criteria, computed as $\frac{\min\{0,\sigma_{22}\}}{\sigma_{22,yc}}$ .
s12_fcs	The principal (w.r.t. directions 1-2) shear stress yielding criteria, computed as $\frac{ \tau_{12} }{\tau_{12,y}}$ .

## 7.5. Modal Data File

The BModes output file has suffix `*_BModes.out`, and it contains the modal displacements and modals slopes computed by the BModes code [2]. The parameters within this file are given in Table 16.

Table 16. BModes Output File Parameters

Parameter	Description
Mode No.	Mode number, a positive integer.
freq	Frequency associated with the following mode shape data [2]. Units [Hz].
span_loc	Span location of a point along the blade pitch axis, measured w.r.t. the blade root and normalized by the blade length [2].
flap disp	Component of modal displacement normal to the blade x-axis [2].
flap slope	Slope of modal displacement curve projected onto a plane that passes through the undeformed blade reference axis (the pitch axis) and is normal to the blade x-axis [2]. Units [rad].
lag disp	Projection of modal displacement in the blade y-direction [2].
lag slope	Slope of modal displacement curve projected in the blade y-direction [2]. Units [rad].
twist	For practical purposes and for modal-based codes such as FAST may be defined as the projection of section twist in a plane that is normal to both the reference plane of rotation and the blade reference axis (usually the pitch axis) [2]. Units [rad].

## 7.6. Optimization Data Files

If requested by the `WRITE_F_ALL` flag, Co-Blade will write the fitness value  $f(\vec{x})$  (as described in Section 6.3), blade mass, penalty factors  $p_1-p_8$ , and 1<sup>st</sup> natural frequency to the output file with suffix `*_F_ALL.out` after every function evaluation. If requested by the `WRITE_X_ALL` or `WRITE_X_ITER` flags, Co-Blade will write the values of the design variables  $\vec{x}$  (as described in Table 11) to the files with suffix `*_X_ALL.out` or `*_X_ITER.out` after each function evaluation or iteration, respectively. These three output files are really only useful for debugging purposes.

## **8. Conclusion and Future Work**

At this time only limited studies have been completed to validate Co-Blade. In previous validation studies, the PreComp code showed excellent agreement for metallic blades with elliptical and rectangular sections for which analytical results could be readily obtained [4, 13]. For the computation of structural properties (such as those listed in Table 12), Co-Blade has shown excellent agreement compared to the PreComp code. One of the limitations of PreComp was that the location of the shear center was computed only approximately, which often lead to inaccurate results for any structural property that also depended on the shear center location [4]. Co-Blade attempts to overcome this limitation by taking a more rigorous approach to computation of the shear center, and also by referencing structural properties to the inertial and centroidal axes which can be computed more accurately than the elastic axes. To validate the computation of effective beam normal stresses Co-Blade has been compared to results from an ANSYS finite element model of a two-material composite rectangular beam. Predictions for the effective beam normal stress have shown satisfactory agreement (with maximum error up to ~7%) between Co-Blade and ANSYS results [12]. The effective beam shear stresses, panel buckling stresses, and lamina level strains and stresses have yet to be compared to any other studies for validation. We hope to fully validate Co-Blade against high fidelity FEM models and experimental data for composite blades (especially anisotropic layups) once such data becomes available. One of the primary motivations for developing Co-Blade was to integrate it with the rotor optimization code HARP\_Opt [3] to perform coupled aerodynamic and structural optimization of turbine blades. We hope to also combine the capabilities of HARP\_Opt and Co-Blade in the near future.

## **Acknowledgements**

The first author thanks the National Science Foundation for providing the Graduate Research Fellowship under Grant No. DGE-0718124. The first author also thanks Matt Trudeau of The Pennsylvania State University for his contributions to this code and for his help in validating some of its results, as well as Alberto Aliseda, Mark Tuttle, and Brian Polagye of the University of Washington for their continued guidance and support. We also gratefully acknowledge Gunjit Bir whose development of the PreComp code helped to inspire this present work.

## **Caveats**

University of Washington does not have the resources to provide full support for this program and do not make any guarantees about the usability or accuracy of Co-Blade, which is essentially a beta code.

## **Feedback**

If you have questions, comments, or suggestions concerning the Co-Blade code please contact Danny Sale.

Danny C. Sale  
Northwest National Marine Renewable Energy Center  
Department of Mechanical Engineering  
University of Washington  
Stevens Way, Box 352600  
Seattle, WA 98195  
phone: (865) 719-0557  
email: [dsale@u.washington.edu](mailto:dsale@u.washington.edu)

## References

- [1] J. M. Jonkman and M. L. Buhl Jr., "FAST User's Guide," NREL/EL-500-29798, National Renewable Energy Laboratory, Golden, CO, 2005.
- [2] G. S. Bir, "User's Guide to BModes: Software for Computing Rotating Beam Couple Modes," NREL TP-500-38976, National Renewable Energy Laboratory, Golden, CO, 2005.
- [3] NWTC Computer-Aided Engineering Tools (HARP\_Opt: An Optimization Code for the Design of Wind and Hydrokinetic Turbines by Danny Sale) [http://wind.nrel.gov/designcodes/simulators/HARP\\_Opt/](http://wind.nrel.gov/designcodes/simulators/HARP_Opt/).
- [4] G. S. Bir, "User's Guide to PreComp: Pre-Processor for Computing Composite Blade Properties," NREL/TP-500-38926, National Renewable Energy Laboratory, Golden, CO, 2005.
- [5] R. M. Jones, *Mechanics of Composite Materials*, McGraw-Hill, 1975.
- [6] M. E. Tuttle, *Structural Analysis of Polymetric Composite Materials*, CRC Press, 2004.
- [7] R. M. Rivello, *Theory and Analysis of Flight Structures*, McGraw-Hill, 1969.
- [8] D. H. Allen and W. E. Haisler, *Introduction to Aerospace Structural Analysis*, John Wiley & Sons, 1985.
- [9] O. A. Bauchau and J. I. Craig, *Structural Analysis: With Applications to Aerospace Structures*, Springer, 2009.
- [10] D. J. Peery and J. J. Azar, *Aircraft Structures*, McGraw-Hill, 2nd edition., 1982.
- [11] W. Young and R. Budynas, *Roark's Formulas for Stress and Strain*, McGraw-Hill, 7th edition, 2001.
- [12] M. G. Trudeau, "Structural and Hydrodynamic Design Optimization Enhancements with Application to Marine Hydrokinetic Turbine Blades," Master's Thesis, The Pennsylvania State University, 2011.
- [13] R. D. Cook and W. C. Young, *Advanced Mechanics of Materials*, Prentice Hall, 2nd edition, 1998.

## Appendix A. Examples of Co-Blade Output Figures

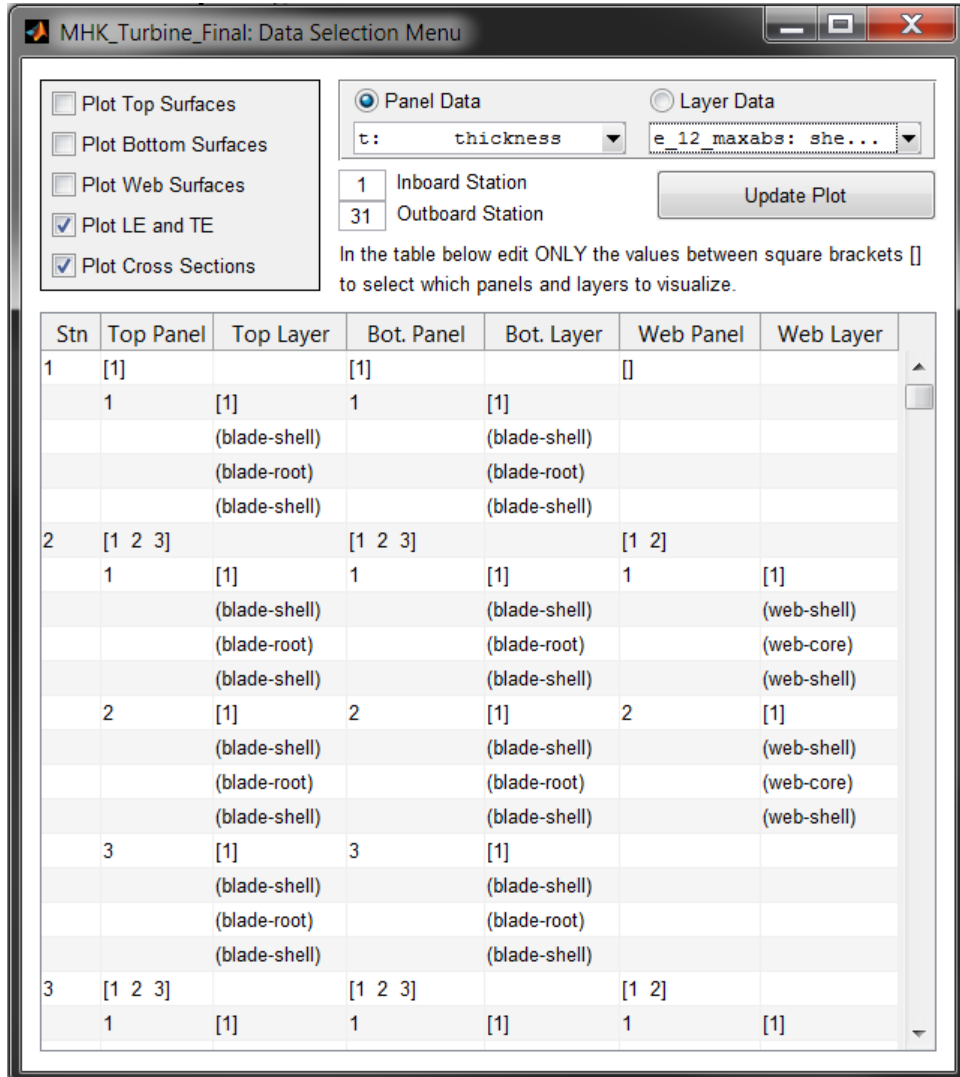


Figure A-1. When DATA\_GUI is set to *true*, this graphical user interface (GUI) is created. This GUI allows the user to plot a 3D representation of the blade and to select via a spreadsheet which panels and/or laminas are shown in the plot. Also, the user can select which output parameter (i.e. Effective modulus, panel thickness, strain, stress, etc.) are visualized in the selected panels and/or laminas.

Many types of visualizations can be created by using this GUI, and some examples are illustrated in Figure A-2 below. The panels and layers which are plotted are selected by editing the values between square brackets (i.e. [ ... ]) in the spreadsheet. It is possible to select one or multiple panels in the editable fields of columns “Top Panel”, “Bottom Panel”, and “Web Panel”. In the editable fields of columns “Top Layer”, “Bottom Layer”, and “Web Layer”, it is only allowable to select a single layer per panel for visualization.

In the example figure shown above, the top surface of the 2<sup>nd</sup> blade station has a total of 3 panels, where each panel has a total of 3 layers per panel. If we only wished to plot the inner-most material layer “blade-shell” in the 2<sup>nd</sup> panel (and ignore plotting of the 1<sup>st</sup> and 3<sup>rd</sup> panels), we would change the editable “Top Panel” field to [2] and the “Top Layer” field for the 2<sup>nd</sup> panel to [3]. The use of this GUI should hopefully be self-explanatory, and some experimentation with the values and observation of the resulting plots should help you learn how to create a variety of visualizations.

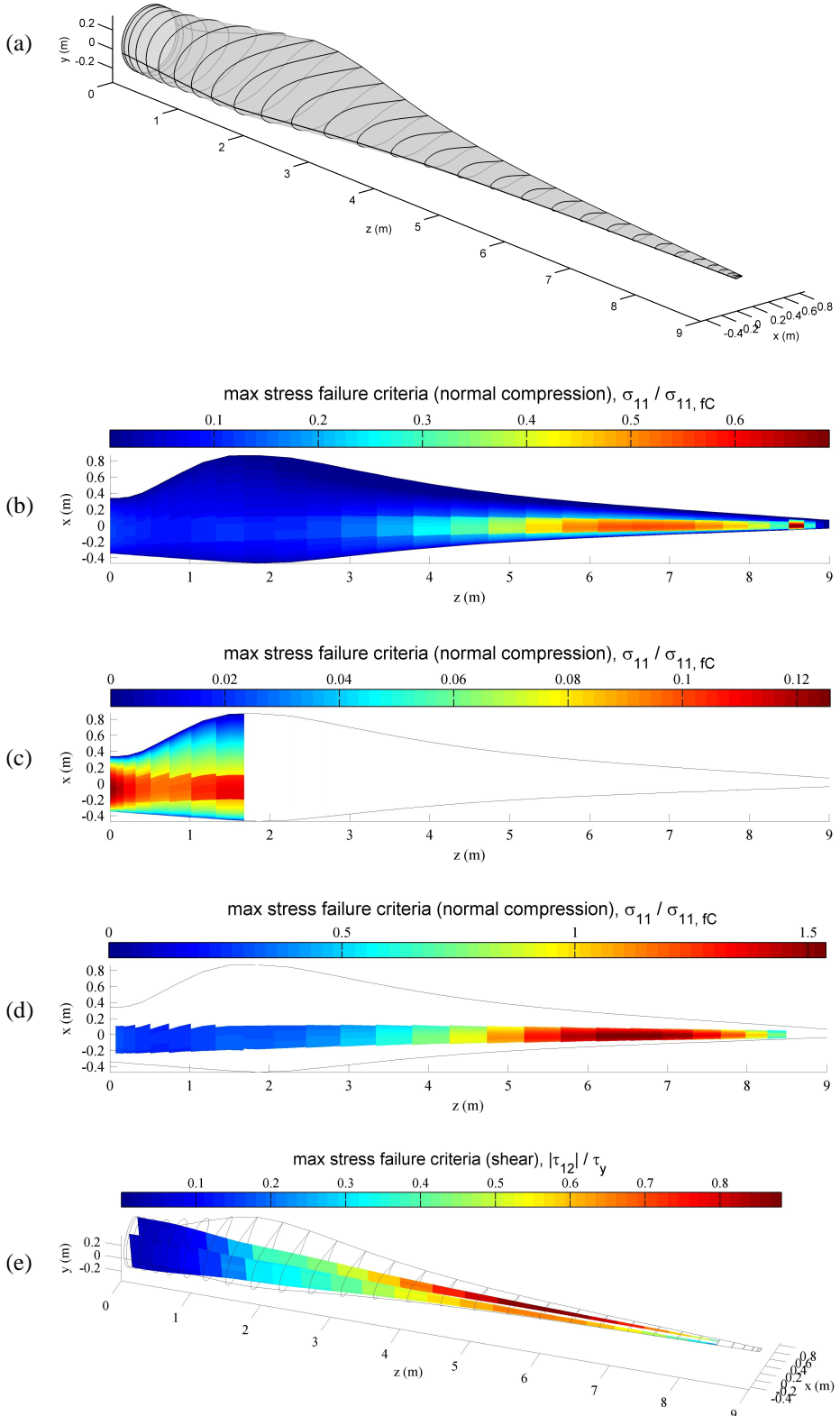


Figure A-2. Some examples of figures that can be created using the graphical user interface (GUI) described in Figure A-1. (a) showing only the external shape of the blade, (b) max stress failure criteria in the “blade-shell” material covering the entire top surface of the blade, (c) max stress failure criteria in the root build-up “blade-root” material, which lies directly under the “blade-shell” material, (d) max stress failure criteria in the spar cap “spar-uni” material, which lies directly under the “blade-root” material, (e) max stress failure criteria in the shear web “web-shell” material. Values greater than 1 for the max stress failure criteria indicate that the material has exceeded its maximum allowable stress.

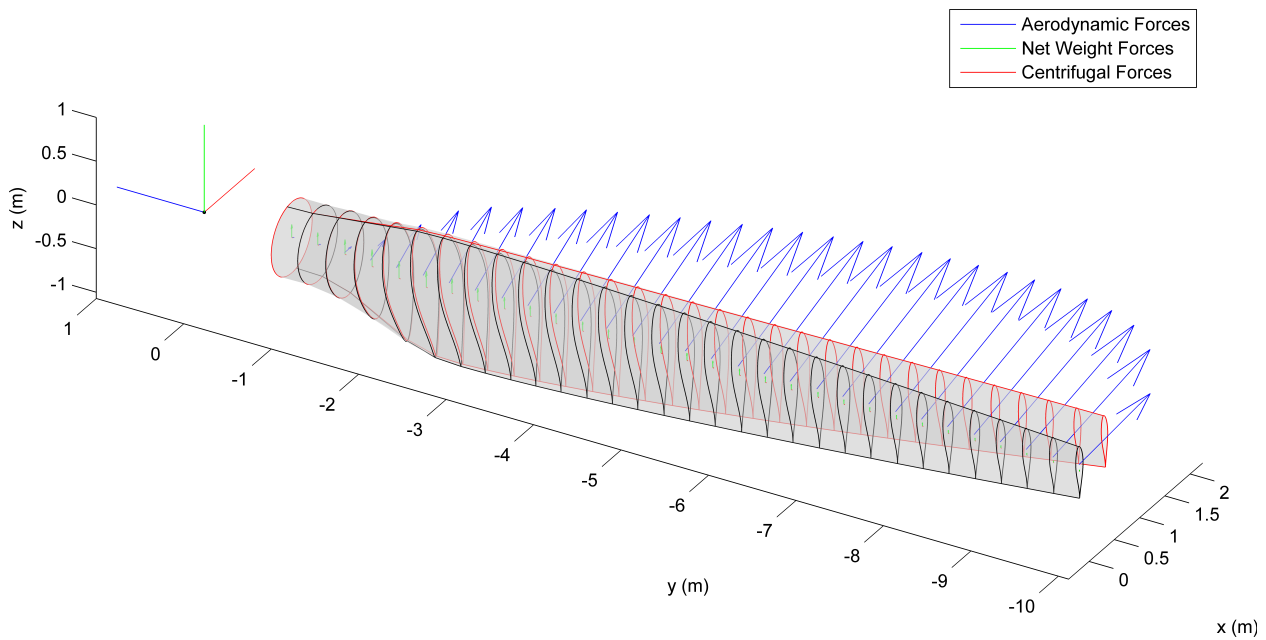


Figure A-3. This figure is created if `PLOT_GBL_SYS = true` and either `PLOT_F_BLD` and/or `PLOT_DISP_BLD` are also `true`. The external blade shape (outlined in black), the displaced external blade shape (outlined in red), and the magnitude and orientation of the applied forces (`px_a`, `py_a`, `px_w`, `py_w`, `pz_w`, `px_c`, `py_c`, and `pz_c`) are plotted in the view of the global coordinate system.

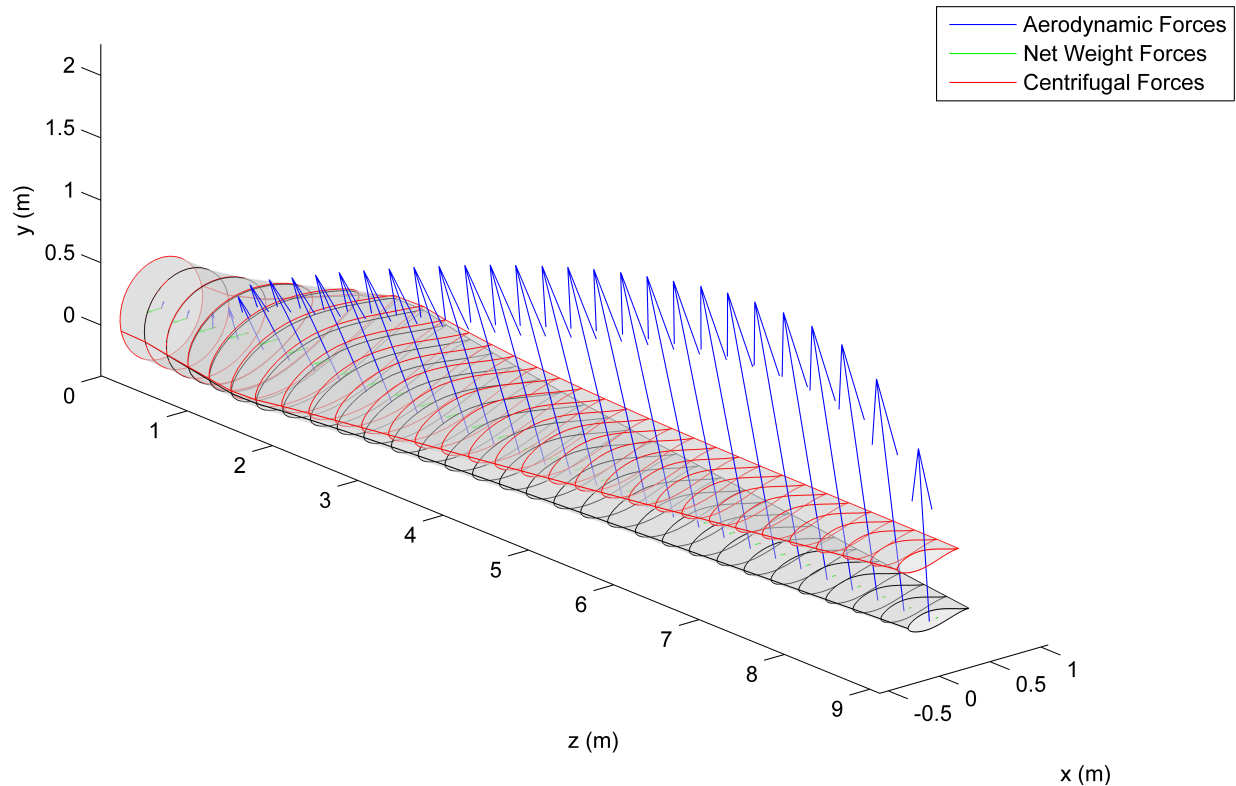


Figure A-4. This figure is created if `PLOT_GBL_SYS = false` and either `PLOT_F_BLD` and/or `PLOT_DISP_BLD` are `true`. It shows the same information as Figure A-3, except plotted in view of the blade coordinate system.

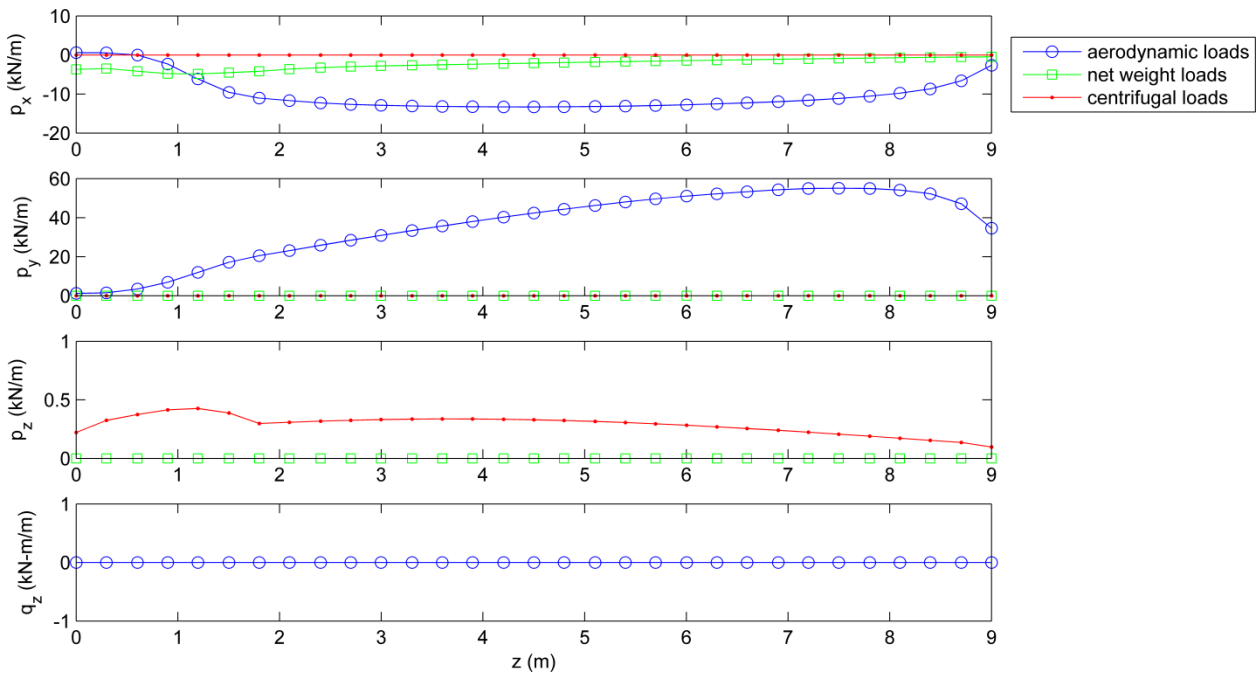


Figure A-5. This figure is created if `PLOT_APPLOADS = true`, showing the aerodynamic forces and moments ( $p_x_a$ ,  $p_y_a$ , and  $q_z_a$ ), the body forces due to net weight ( $p_x_w$ ,  $p_y_w$ , and  $p_z_w$ ), and the body forces due to centrifugal force ( $p_x_c$ ,  $p_y_c$ , and  $p_z_c$ )—w.r.t. the blade coordinate system.

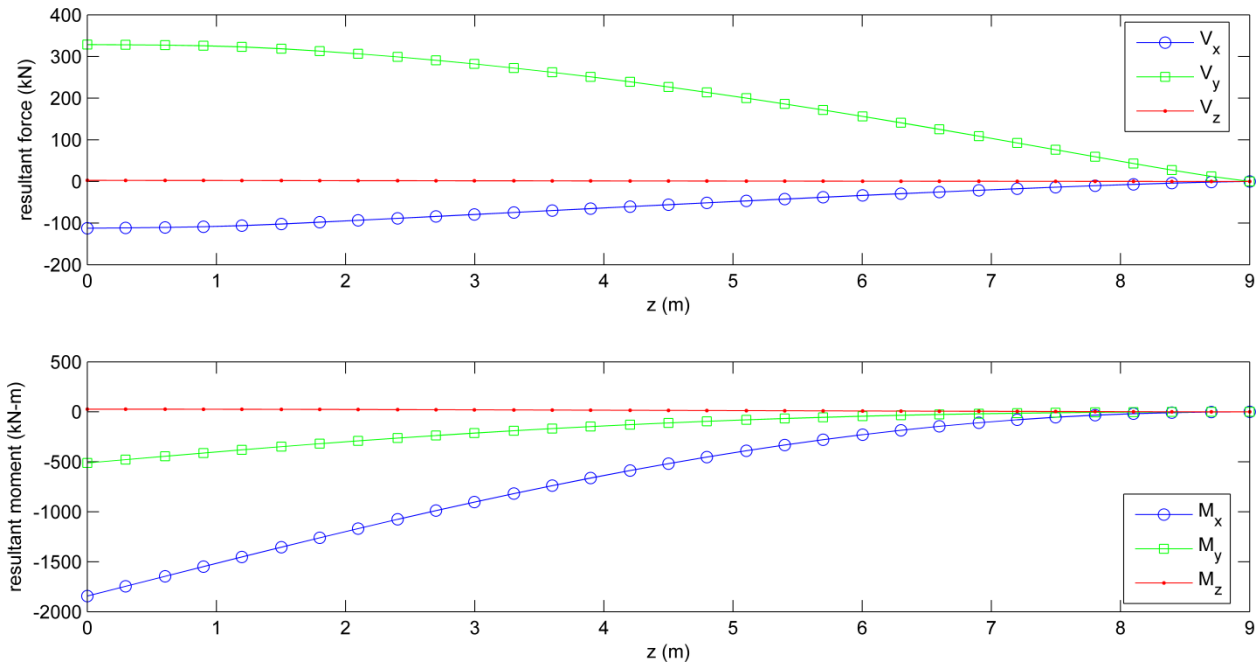


Figure A-6. This figure is created if `PLOT_RESLOADS = true`, showing the resultant shear forces ( $V_x$ ,  $V_y$ , and  $V_z$ ), resultant bending moments ( $M_x$  and  $M_y$ ), and resultant torsional moment ( $M_z$ ) along the blade length. Note: these resultant forces and moments are defined w.r.t. to the blade centroidal axis (i.e. the axis intersecting the locus of tension centers, but where the x-y axes of the centroidal axis are still parallel and perpendicular to the x-y axes of the blade coordinate system).

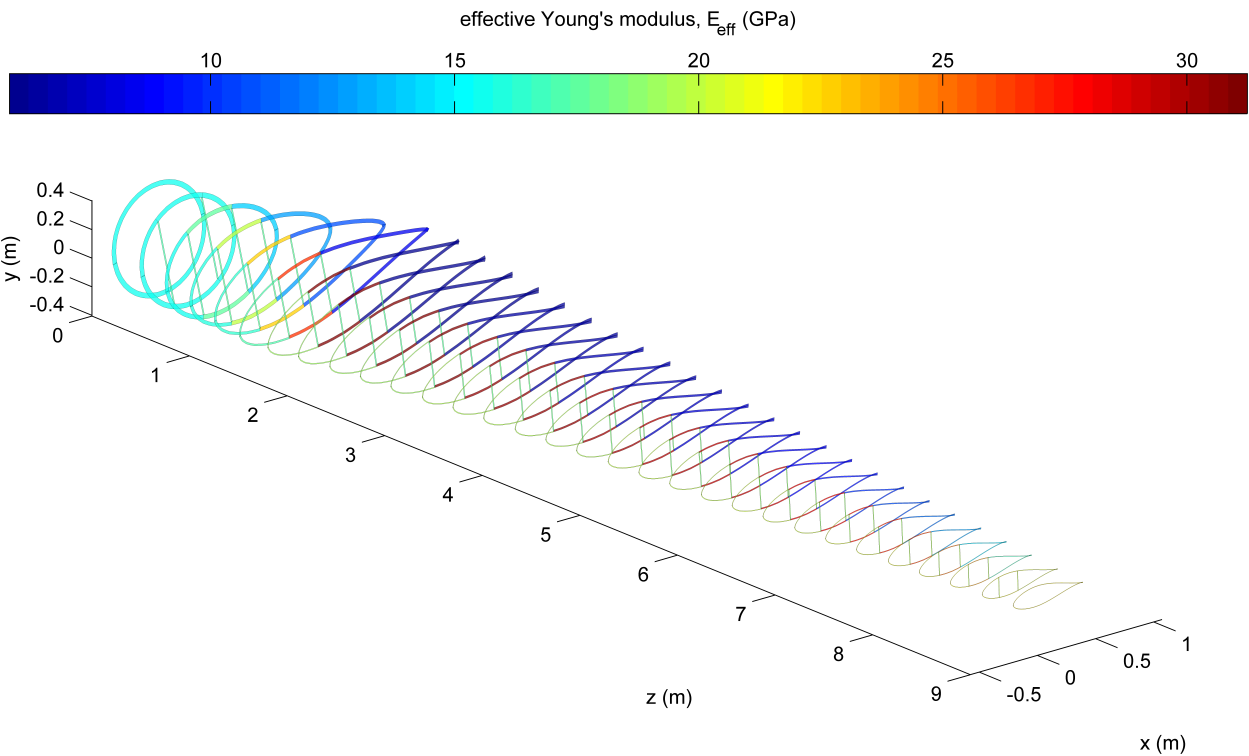


Figure A-7. This figure is created if `PLOT_YMOD = true`, showing the three-dimensional blade geometry with the panel laminates colored by their effective Young's modulus ( $E_{\text{eff}}$ ) in view of the blade coordinate system.

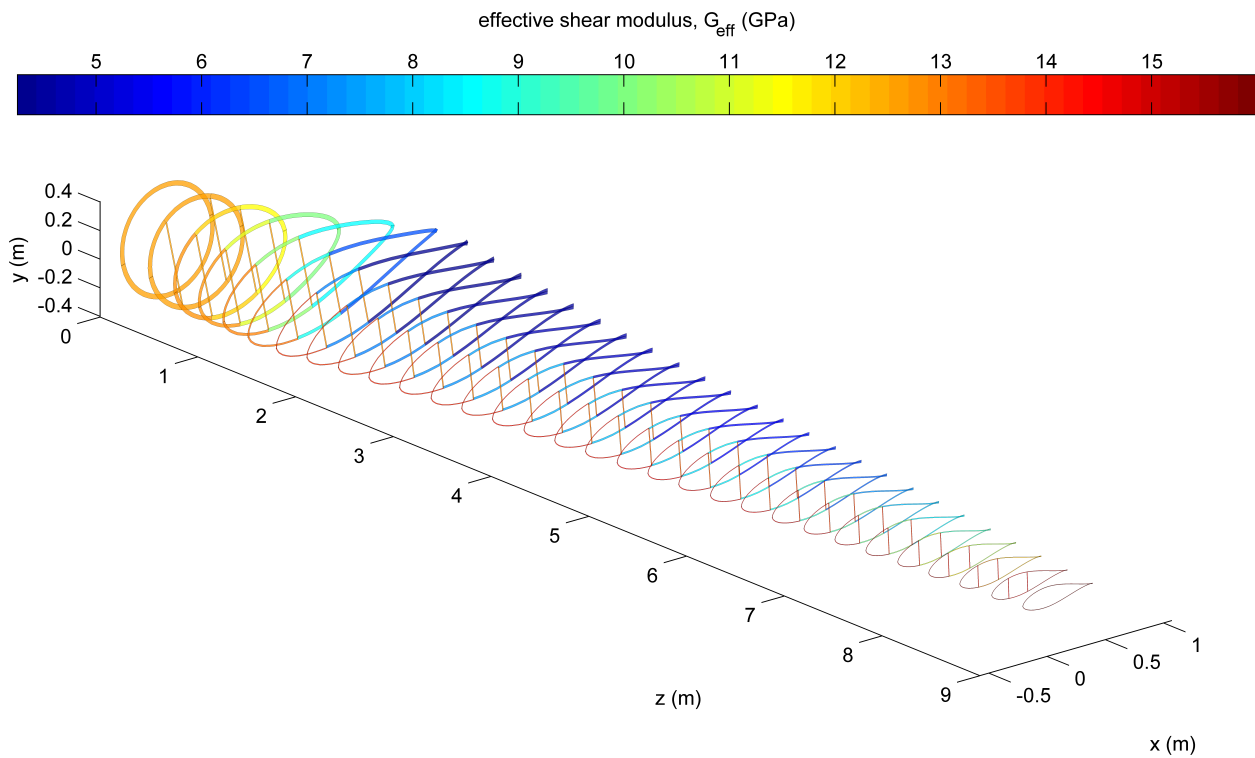


Figure A-8. This figure is created if `PLOT_GMOD = true`, showing the three-dimensional blade geometry with the panel laminates colored by their effective shear modulus ( $G_{\text{eff}}$ ) in view of the blade coordinate system.

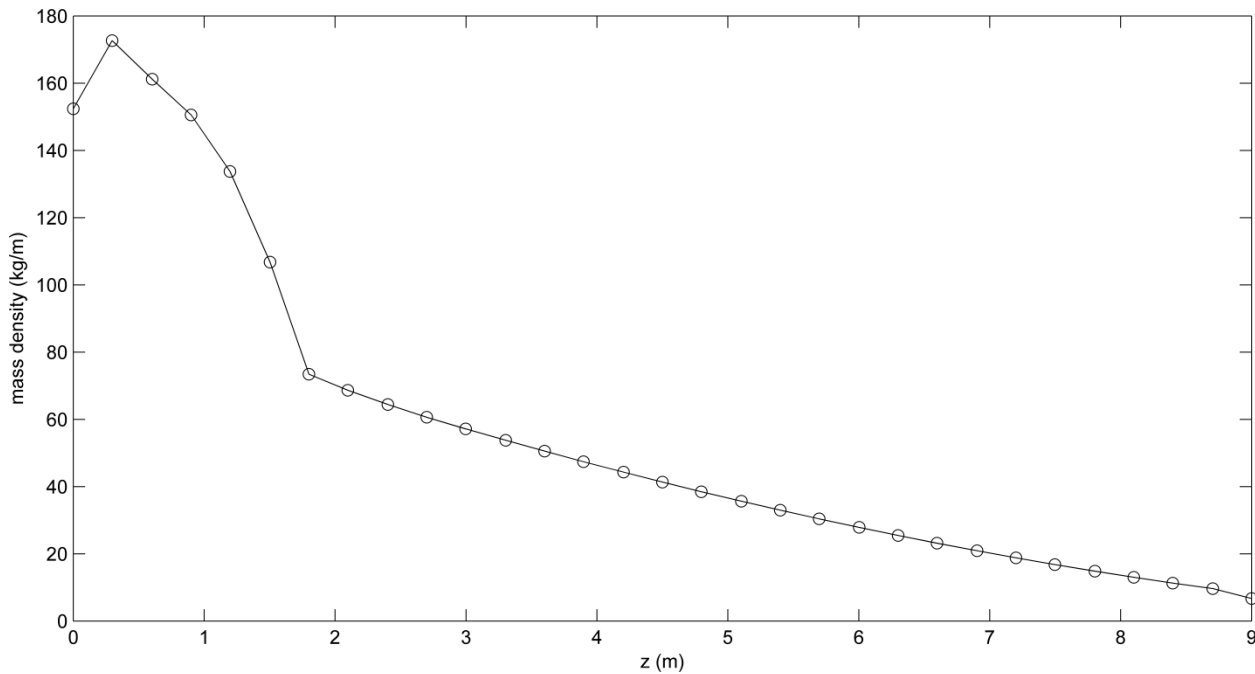


Figure A-9. This figure is created if `PLOT_MASS_DEN = true`, showing the section mass per unit length (`mass_den`) along the blade length (`z`).

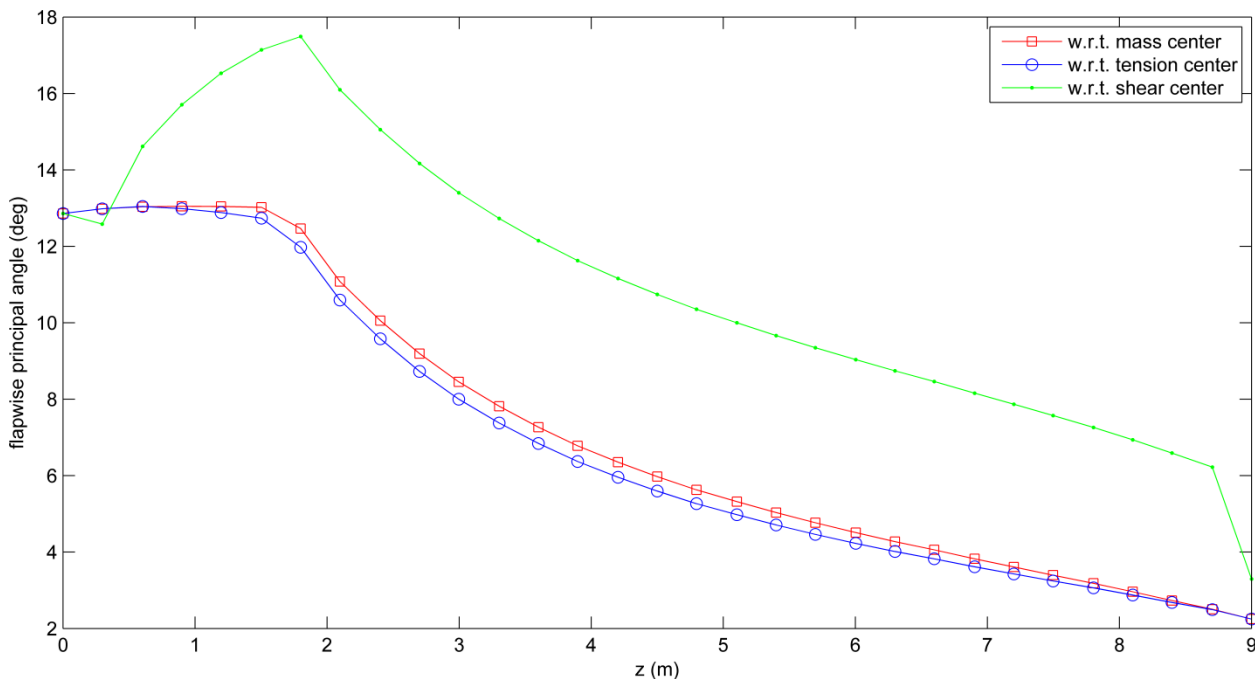


Figure A-10. This figure is created if `PLOT_PRIN_ANG = true`, showing the angle between the blade coordinate system x-axis and the principal flapwise axis w.r.t. the mass center, tension center, and shear center: (`iner_tw`), (`cent_tw`), and (`elas_tw`), respectively.

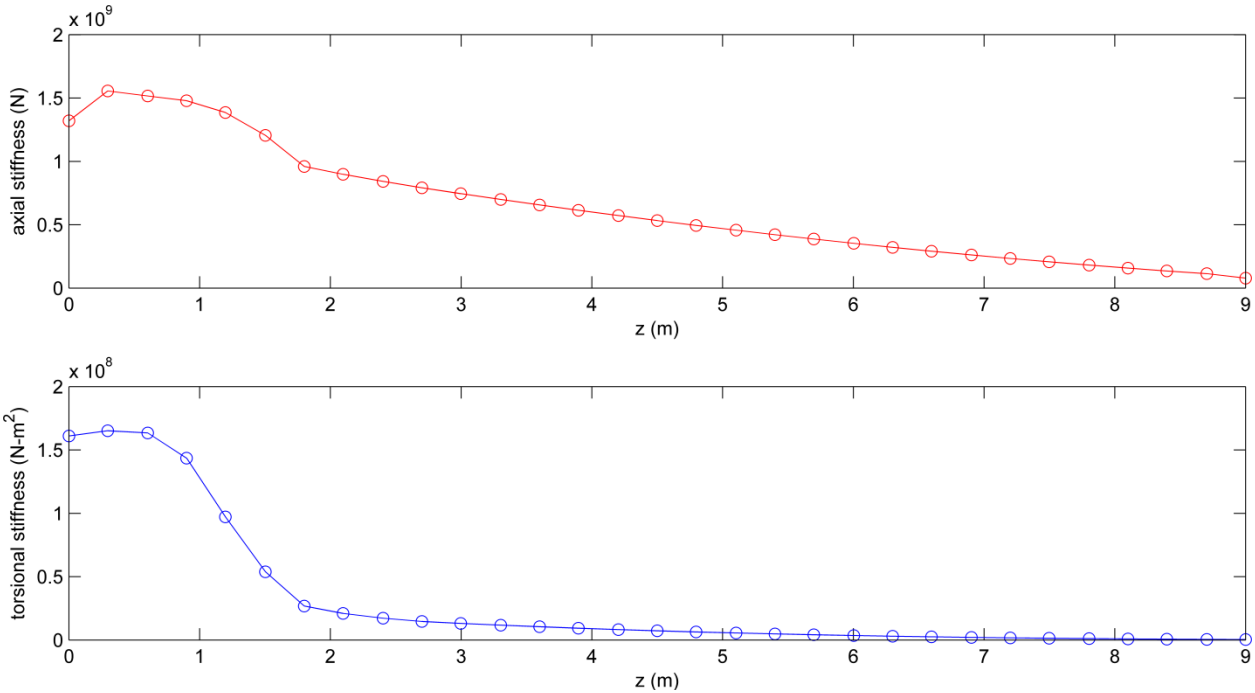


Figure A-11. This figure is created if `PLOT_AT_STFF = true`, showing the axial stiffness (`axial_stff`) and torsional stiffness (`tor_stff`) along the length of the blade.

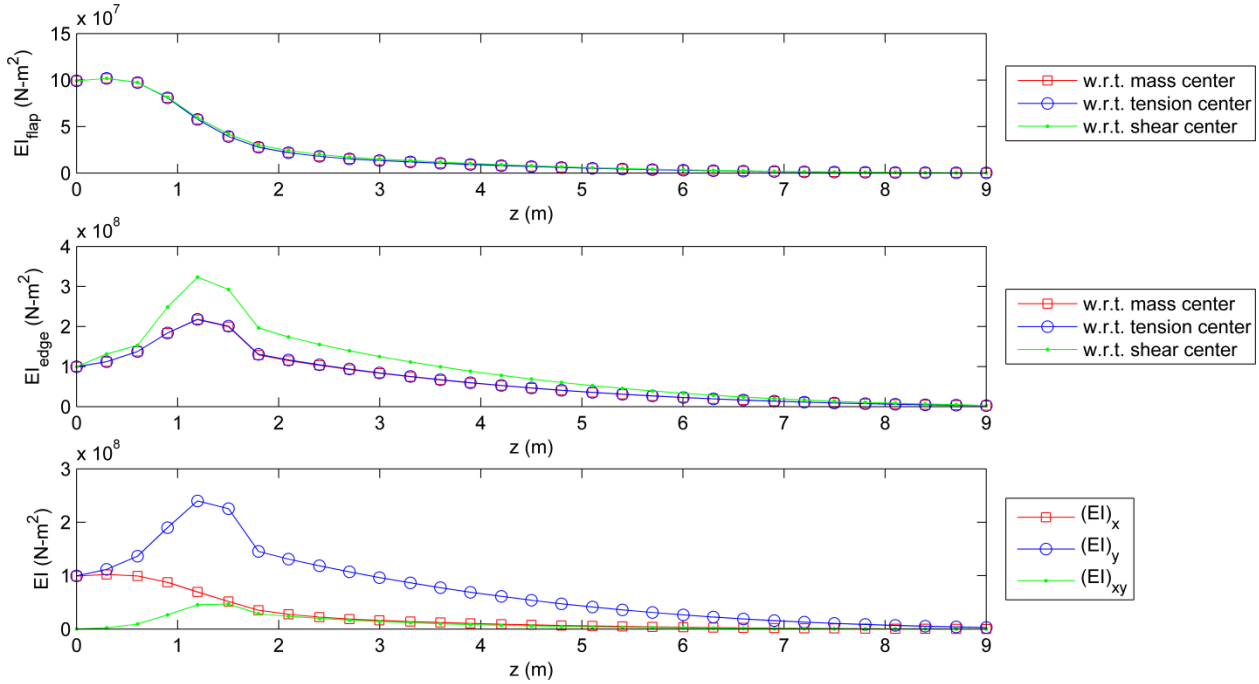


Figure A-12. This figure is created if `PLOT_BSTFF = true`, showing the principal flapwise and edgewise bending stiffnesses along the length of the blade w.r.t. the mass center, tension center, and shear center: (`flapEI_cm` and `edgeEI_cm`), (`flapEI_tc` and `edgeEI_tc`), and (`flapEI_sc` and `edgeEI_sc`), respectively. The bending stiffnesses w.r.t. the blade coordinate system x- and y-axis, and the cross bending stiffness are also shown: (`EIx`), (`EIy`), and (`EIxy`), respectively.

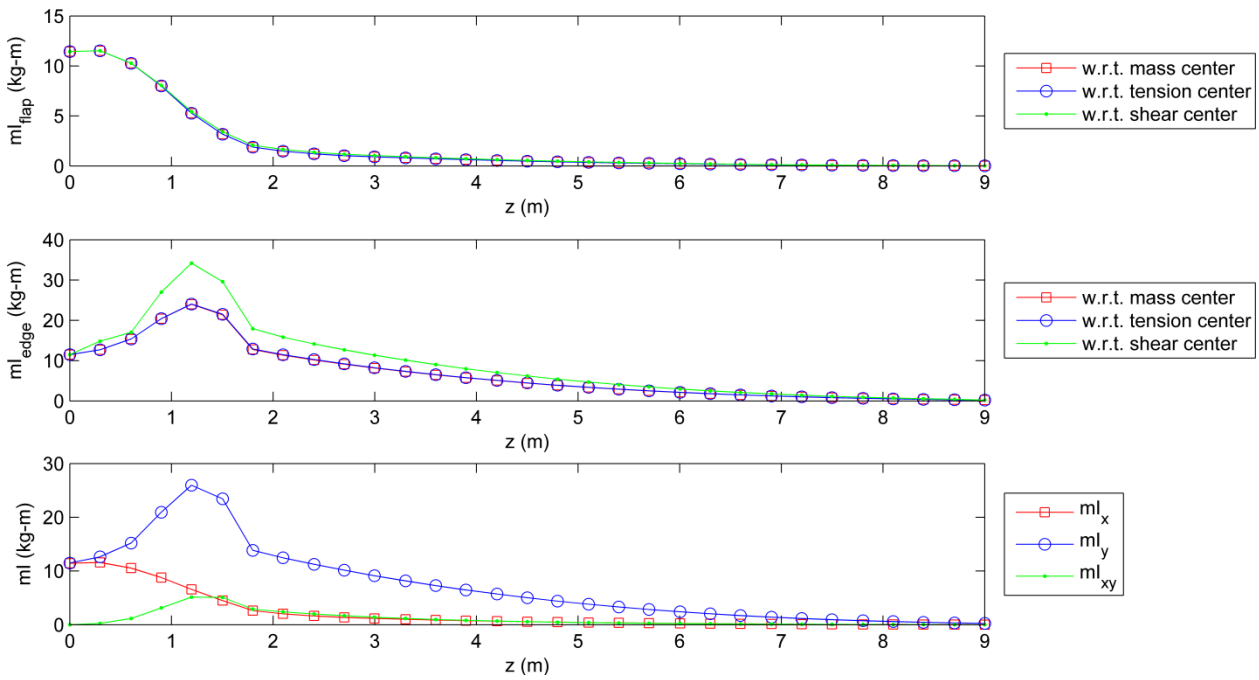


Figure A-13. This figure is created if `PLOT_INER = true`, showing the principal flapwise and edgewise mass moments of inertia per unit length along the length of the blade w.r.t. the mass center, tension center, and shear center: (`flapIner_cm` and `edgeIner_cm`), (`flapIner_tc` and `edgeIner_tc`), and (`flapIner_sc` and `edgeIner_sc`), respectively. The mass moments of inertia per unit length w.r.t. the blade x- and y-axis, and the product mass moment of inertia per unit length are also shown: (`mlx`), (`mly`), and (`mlxy`), respectively.

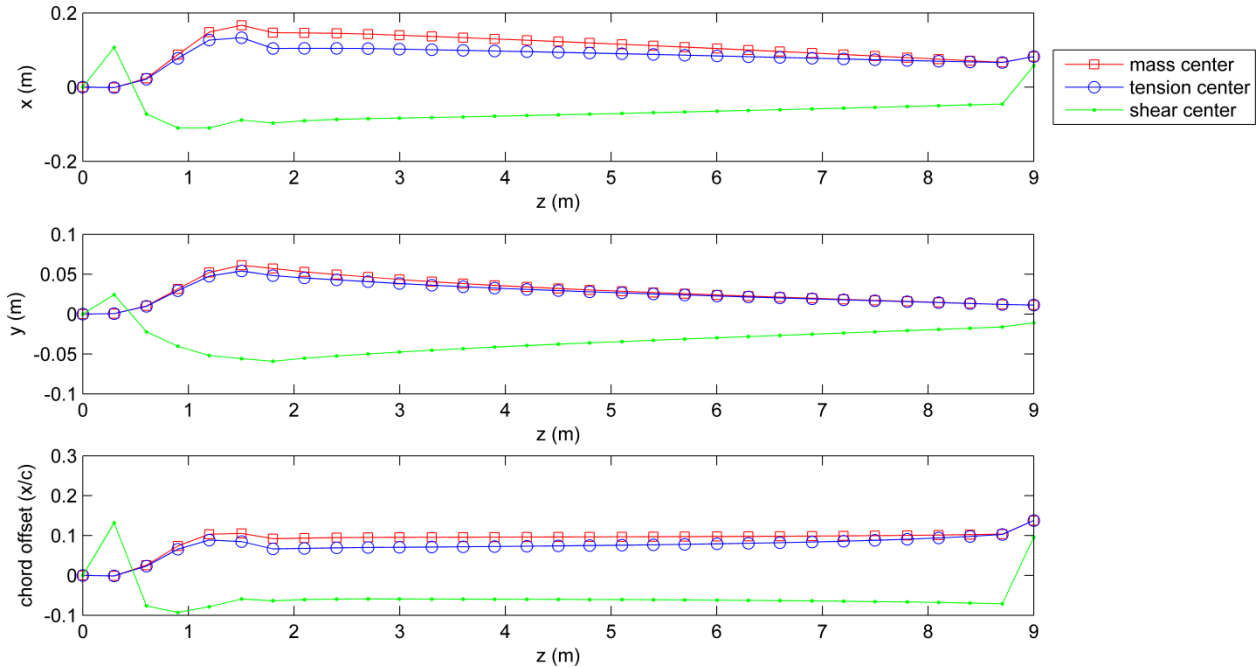


Figure A-14. This figure is created if `PLOT_CENTERS = true`, showing the  $(x, y)$  coordinates of the center of mass, tension center, and shear center: (`x_cm`, `y_cm`), (`x_tc`, `y_tc`), and (`x_sc`, `y_sc`), respectively. Also shown are the chordwise offsets from the pitch axis for the center of mass (`cm_offset`), tension center (`tc_offset`), and shear center (`sc_offset`).

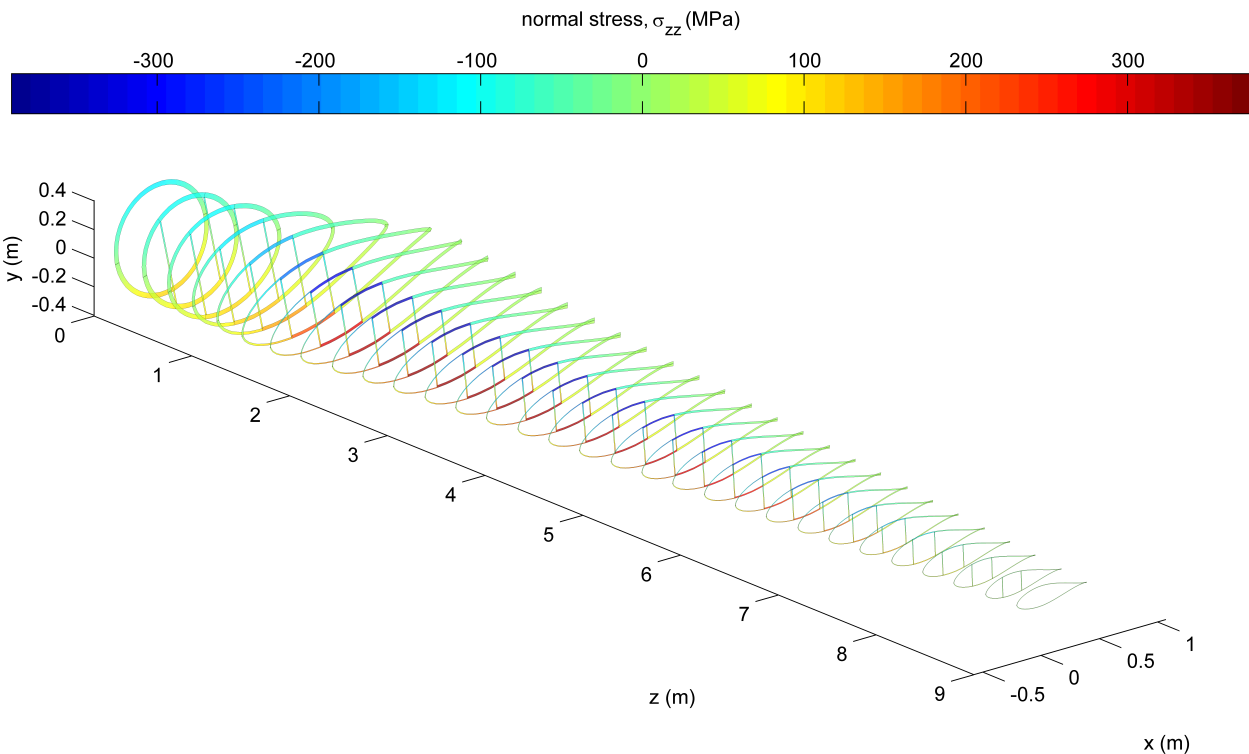


Figure A-15. This figure is created if `PLOT_NORMS = true`, showing the three-dimensional blade geometry with the panel laminates colored by their effective beam normal stress ( $\sigma_{zz}$ ) in view of the blade coordinate system.

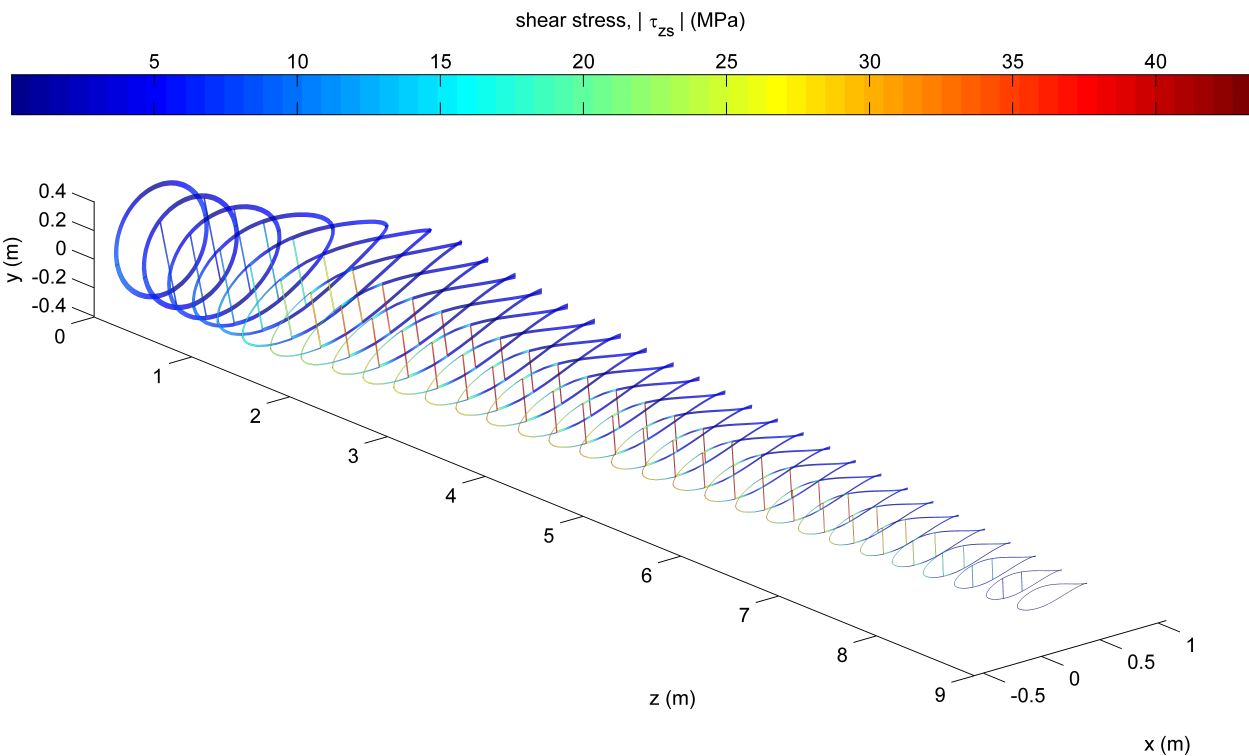


Figure A-16. This figure is created if `PLOT_SHEARS = true`, showing the three-dimensional blade geometry with the panel laminates colored by their effective beam shear stress ( $|\tau_{zs}|$ ) in view of the blade coordinate system.

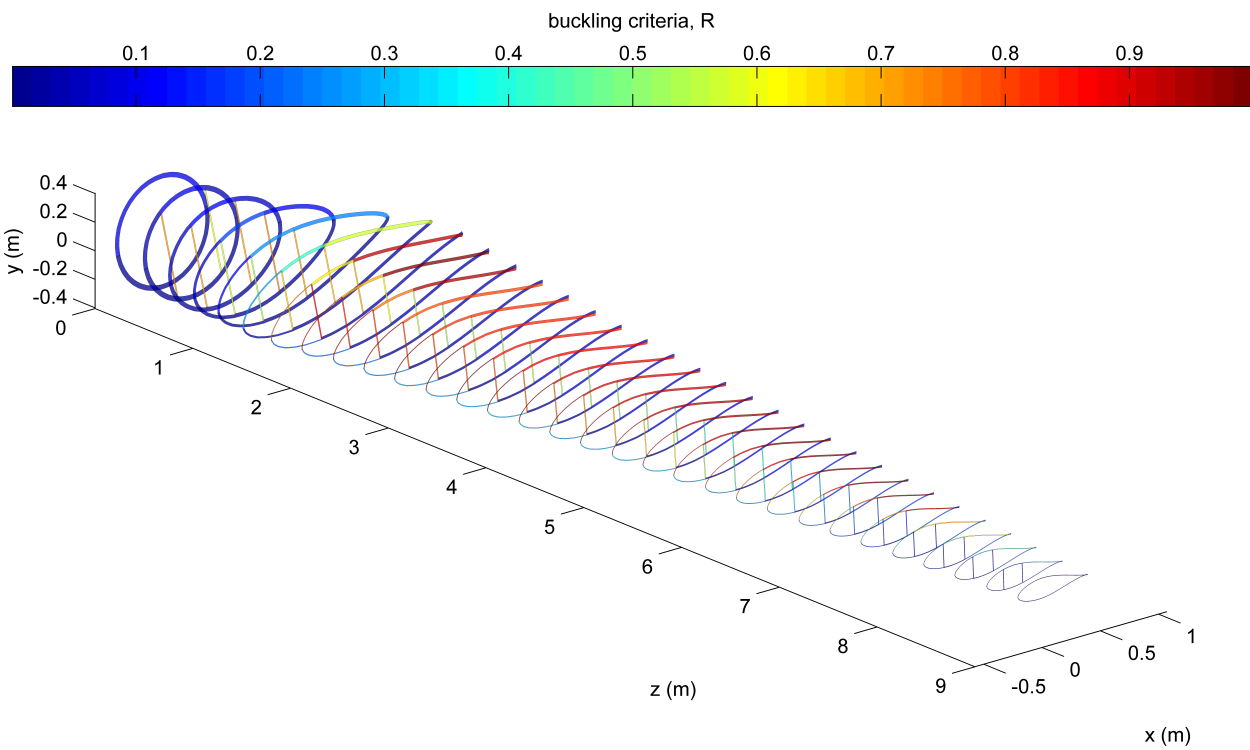


Figure A-17. This figure is created if `PLOT_BCRIT = true`, showing the three-dimensional blade geometry with the panel laminates colored by their panel buckling criteria (`buckleCrit`). A buckling criteria greater than 1 indicates that the panel has buckled under the combined effect of compression and shear, while a ratio less than 1 indicates that the panel has not buckled. Refer to Table 14 and [10, 11] for explanation of how the buckling criteria is computed for the top, bottom, and web panels.

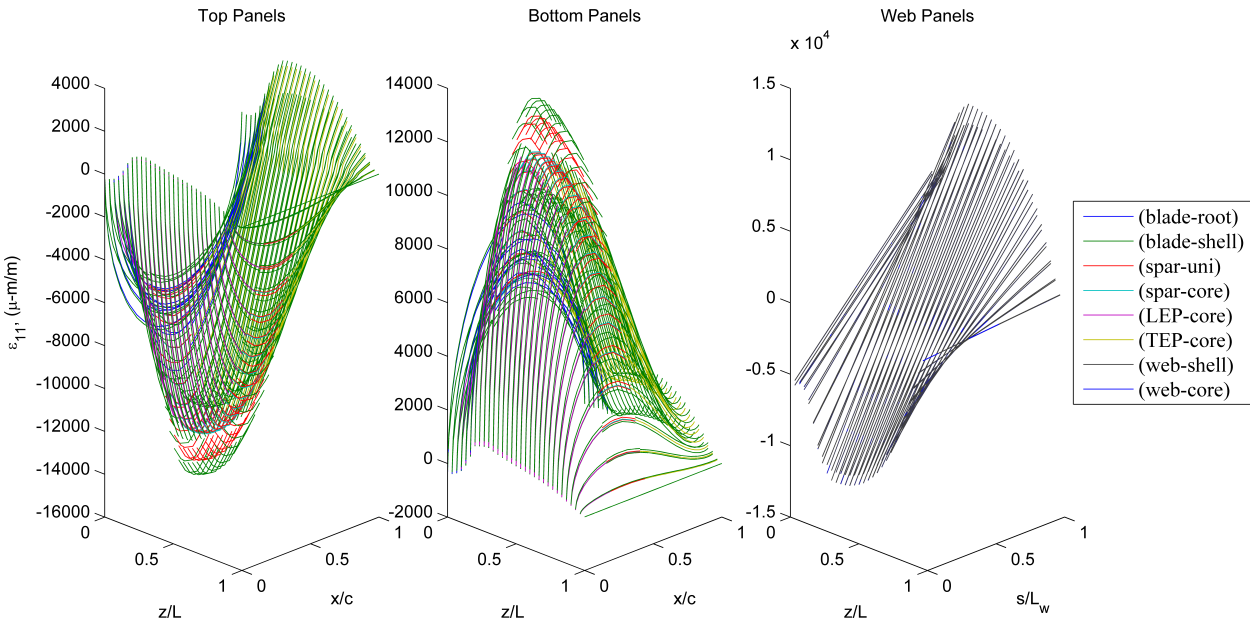


Figure A-18. This figure is created if `PLOT_E11 = true`, showing the span variant and chordwise variant normal strains in direction-1 (the principal direction) within each individual lamina of the top, bottom, and web panels. The coordinate  $z/L$  is the distance measured along the blade pitch axis starting at the blade root and normalized by the blade length. The coordinate  $x/c$  is the distance measured along the chord line starting at the leading edge and normalized by the chord. The coordinate  $s/L_w$  is the distance measured along the mid-wall of the web starting at the end of the web connected to the top surface and normalized by the total length of the web panel. A line is plotted for every single lamina within the entire blade, and the lines are color coded by their material name. This plot can become easily cluttered, but it provides a quick reference for the range of lamina strain magnitudes within the entire blade. A similar plot can be created for the other strain components,  $\epsilon_{22}$  and  $\gamma_{12}$ , by the `PLOT_E22` and `PLOT_E12` flags.

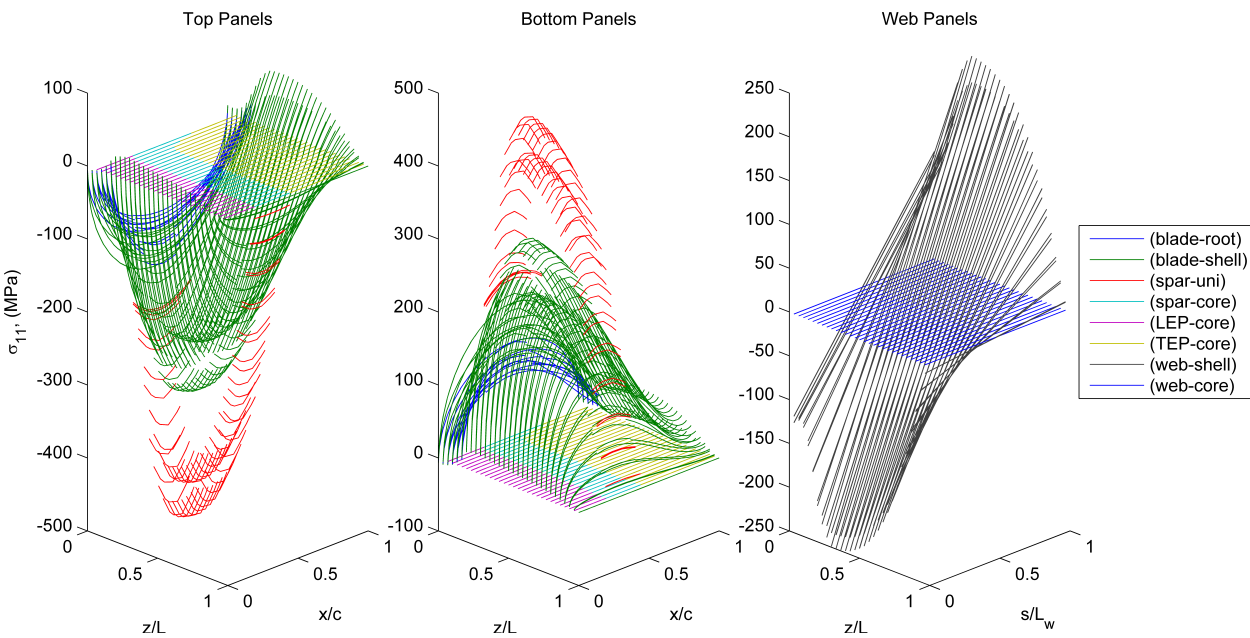


Figure A-19. This figure is created if `PLOT_S11 = true`, showing the span variant and chordwise variant normal stresses in direction-1 (the principal direction) within each individual lamina of the top, bottom, and web panels. This plot is similar to Figure A-18, except showing the lamina stress  $\sigma_{11}$ . A similar plot can be created for the other stress components,  $\sigma_{22}$  and  $\tau_{12}$ , by the `PLOT_S22` and `PLOT_S12` flags.

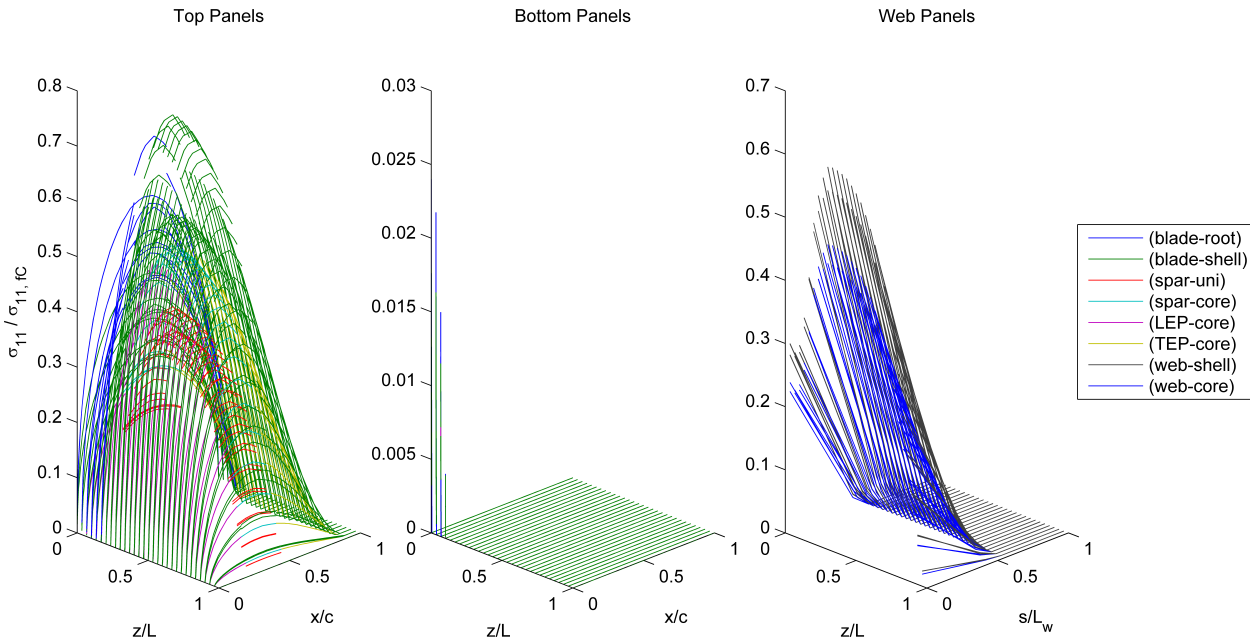


Figure A-20. This figure is created if `PLOT_S11_FC = true`, (similar to Figure A-18) showing the span variant and chordwise variant compressive failure criteria for the normal stresses in direction-1 (the principal direction) within each individual lamina of the top, bottom, and web panels—computed as  $\frac{\min\{0,\sigma_{11}\}}{\sigma_{11,fc}}$ . A similar plot can be created for the other stress component,  $\frac{\min\{0,\sigma_{22}\}}{\sigma_{22,yc}}$ , by the `PLOT_S22_FC` flag. This plot can become easily cluttered, but it provides a quick reference for the range of lamina stress magnitudes within the entire blade.

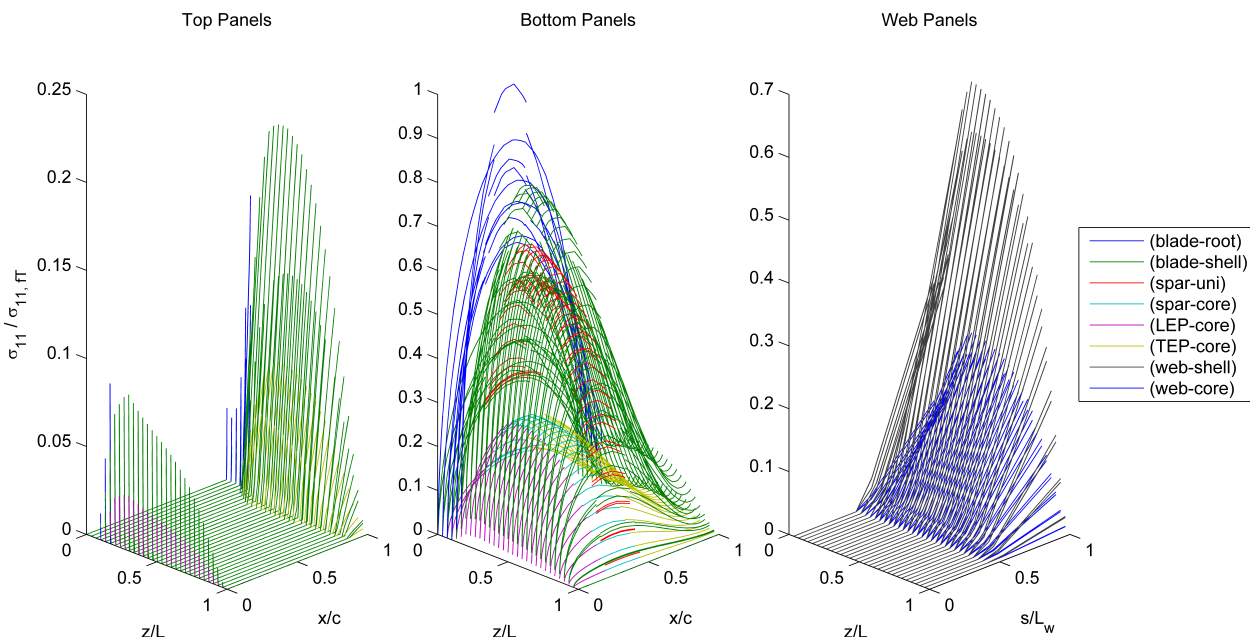


Figure A-21. This figure is created if `PLOT_S11_FC = true`, (similar to Figure A-18) showing the span variant and chordwise variant tensile failure criteria for the normal stresses in direction-1 (the principal direction) within each individual lamina of the top, bottom, and web panels—computed as  $\frac{\max\{0,\sigma_{11}\}}{\sigma_{11,ft}}$ . A similar plot can be created for the other stress component,  $\frac{\max\{0,\sigma_{22}\}}{\sigma_{22,yt}}$ , by the `PLOT_S22_FC` flag. This plot can become easily cluttered, but it provides a quick reference for the range of lamina stress magnitudes within the entire blade.

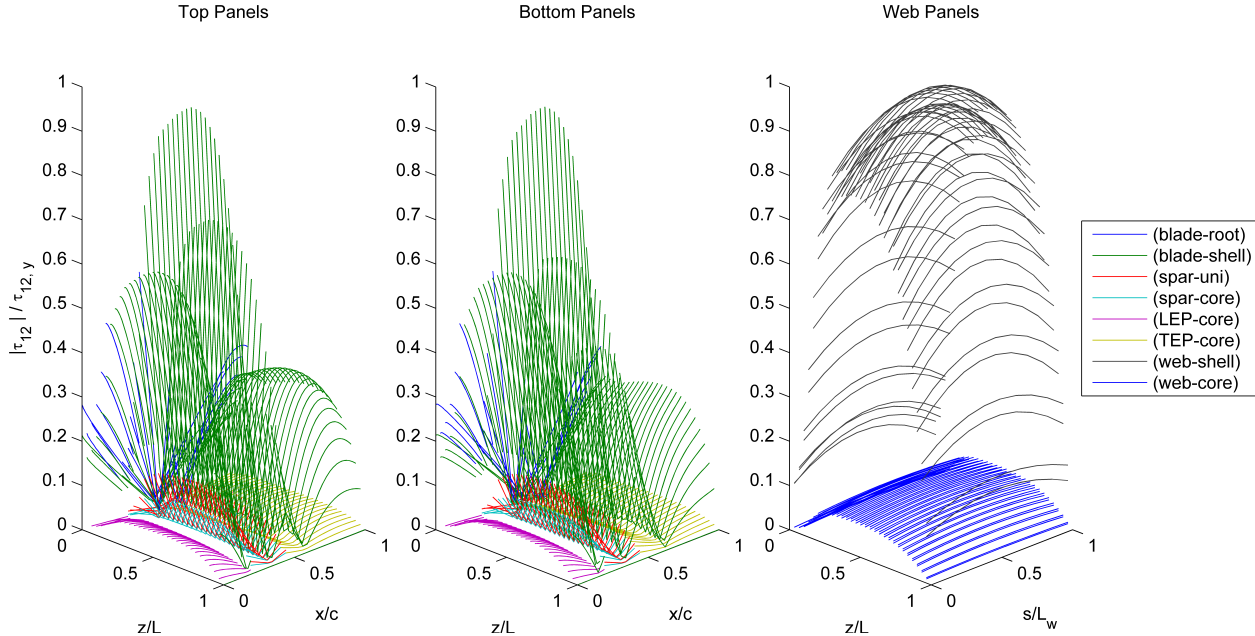


Figure A-22. This figure is created if `PLOT_S12_FC = true`, (similar to Figure A-18) showing the span variant and chordwise variant yielding criteria for the principal shear stresses (w.r.t. the principal directions 1-2) within each individual lamina of the top, bottom, and web panels—computed as  $\frac{|\tau_{12}|}{\tau_{12,y}}$ . The discontinuities that are seen in the shear stress occur where a shear web intersects the top and bottom panels, or when a sudden change in wall thickness or elastic modulii occurs. This plot can become easily cluttered, but it provides a quick reference for the range of lamina stress magnitudes within the entire blade.

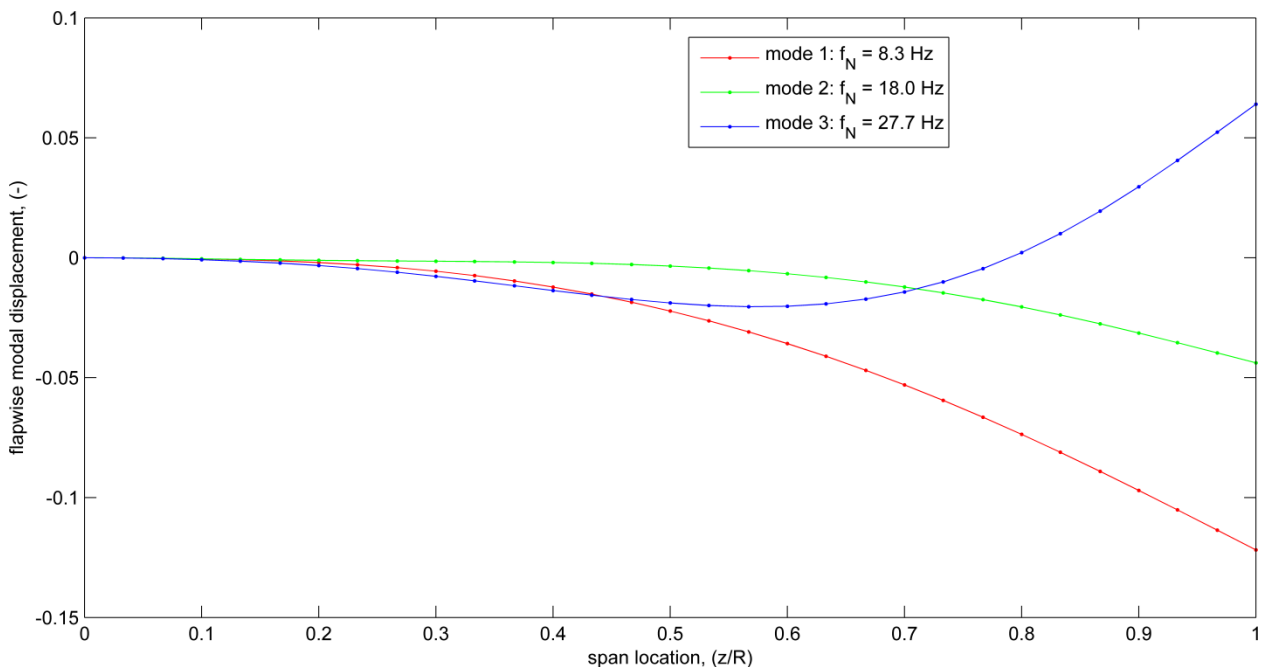


Figure A-23. This figure is created if `PLOT_MODE_D = true`, showing the flapwise modal displacements (`flap_disp`) along the fraction of the blade length (`span_loc`) for the corresponding frequencies (`freq`). If `PLOT_MODE_D = true`, similar figures will also be created showing the edgewise modal displacement (`lag_disp`), flapwise and edgewise modal slopes (`flap_slope` and `lag_slope`), and modal twist (`twist`).

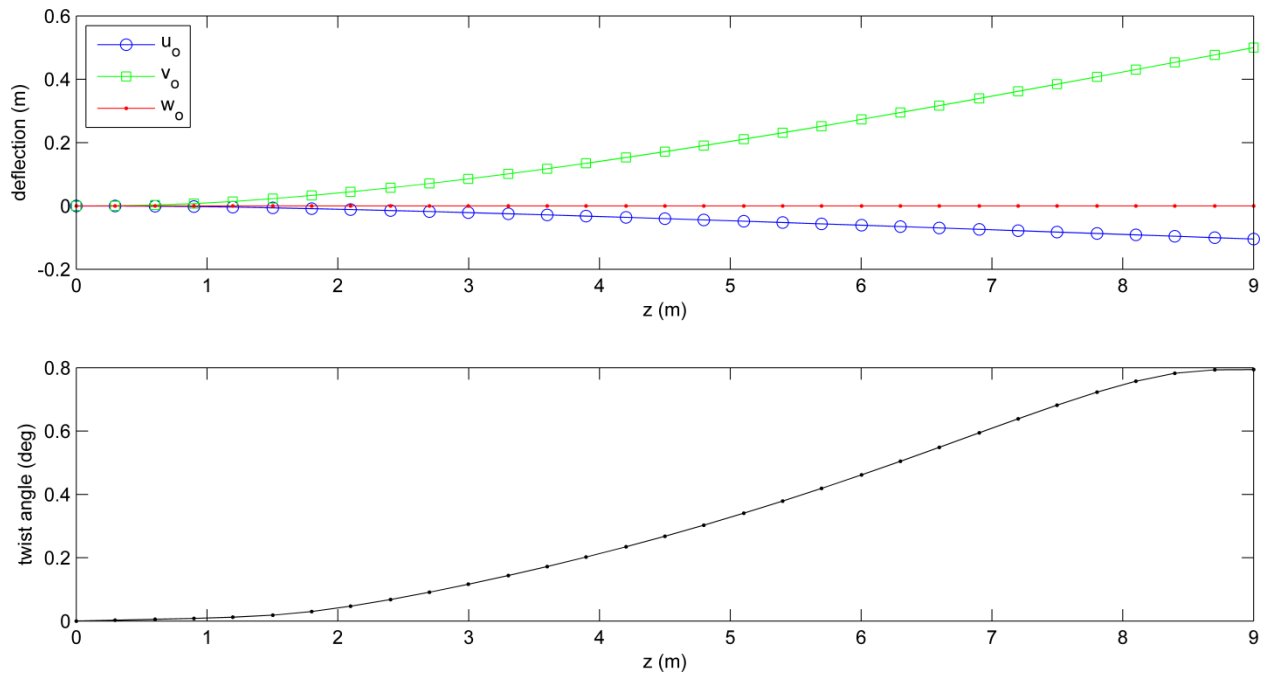


Figure A-24. This figure is created if `PLOT_DEFLECT = true`, showing the displacements in the x-, y-, and z-directions along the blade centroidal axis:  $(u_o)$ ,  $(v_o)$ , and  $(w_o)$ , respectively. Also shown is the rigid body rotation angle of twist about the shear center ( $\tau_z$ ) along the blade length.